Prion protein aggregation

Shweta Jain and Jayant B. Udgaonkar*

National Centre for Biological Sciences, Tata Institute of Fundamental Research, Bangalore 560 065, India

Prion protein-mediated disorders appear to originate from the aggregation reactions of the prion protein. Like other amyloidogenic proteins, prion proteins form a range of fibrillar morphologies. The pre-fibrillar forms seen at the beginning of the reaction are also heterogeneous; hence it appears that structural heterogeneity sets in early during the aggregation reaction. The prion protein aggregation may therefore proceed from many different precursor states, and structural heterogeneity in prion fibrils might originate from the utilization of distinct nucleation and elongation mechanisms. This review discusses the current understanding of the structural heterogeneity inherent in the aggregation reactions of prion proteins. It examines how an understanding of the structural and mechanistic basis of prion protein aggregation can provide molecular-level insights into the characteristic features of prion disorders, namely the infectious nature of the prion protein, prion strain phenomena and species barriers.

Keywords: Alternative pathways, amyloid fibrils, oligomers, prion protein, structural heterogeneity.

THE prion protein (PrP) is a highly conserved glycoprotein, which is expressed ubiquitously in the mammalian brain, specifically in neurons[1–3]. It is composed of two domains[4], is anchored to the cell membrane through a C-terminal glycophosphatidylinositol (GPI) anchor, and is also glycosylated at two asparagine residues. The N-terminal domain is largely disordered, and has 4–5 octa-peptide repeats (Figure 1 *a*). It has a high affinity for divalent metal ions, such as Cu^{2+}, and becomes partially structured upon interaction with Cu^{2+} (refs 5–7). The C-terminal portion is structured, consists of three long α-helices and two small β-strands, and has a disulphide bond that links helices 2 and 3 (Figure 1 *a* and *b*).

The exact biological function of the prion protein is unknown. It has, however, been linked to multiple physiological processes[8,9]. An alternative, non-native conformation of the prion protein, PrP^{Sc}, is infectious, and causes prion diseases[10,11], a group of fatal neurodegenerative diseases, which include Creutzfeldt-Jakob disease (CJD), fatal familial insomnia (FFI), mad cow disease and scrapie.

*For correspondence. (e-mail: jayant@ncbs.res.in)

Discovery of the prion

The cause of CJD was unknown for many years. The disease was known to progress fast, after onset, causing death within a few months without invoking any immune response[12–14]. Similarities between CJD and Kuru in humans[15], and also between Kuru in humans and scrapie in sheep[16], became evident. Upon vaccination of sheep against scrapie, using a formalin-treated suspension of ovine brain and spleen, the sheep, instead of developing immunity against scrapie, succumbed to the disease[17], suggesting that the pathogen is resistant to formalin and heat. It was proposed that scrapie is caused by a 'slow

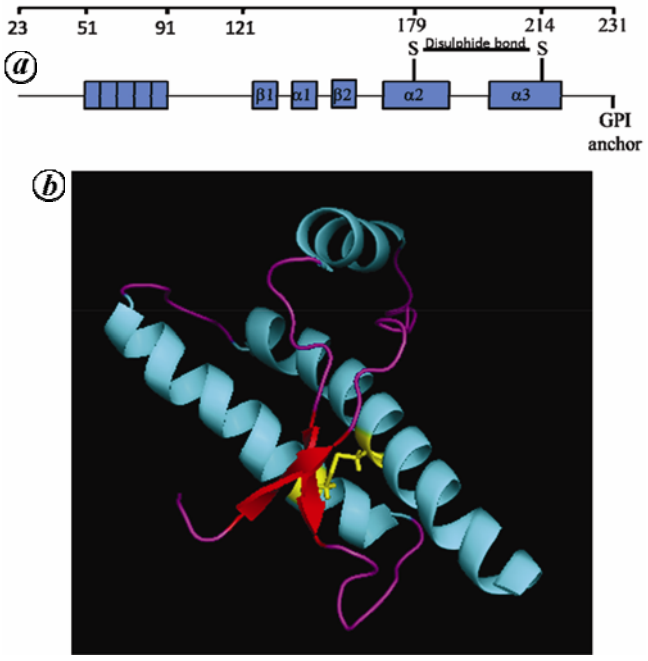

Figure 1. Schematic of the full length mammalian prion protein (PrP) and NMR structure of C-terminal folded domain of PrP. ***a***, Primary structure of the cellular prion protein (PrP^{C}). The full length mammalian prion protein has 209 amino acid residues, and consists of two domains. The N-terminal domain (23–120) is unstructured and contains 4–5 octapeptide repeats, shown in blue boxes between residues 51 and 91. The C-terminal domain (121–231) is folded into two small β-strands and three α-helices. This protein is anchored to the cell membrane by a glycosylphosphatidylinositol (GPI) anchor at the C-terminus. There are two glycosylation sites, at residues 181 and 197. A disulphide bond links α-helix 2 to α-helix 3. ***b***, NMR structure of the folded C-terminal domain (residues 121–231) of the recombinant human prion protein. The disulphide bond linking α-helix 2 to α-helix 3 is shown in yellow. The structure has been drawn from the PDB entry 1QM3, using PyMOL (http://www.pymol.org).

virus'[18]. Along similar lines, it was proposed that Kuru is also transmissible like scrapie, and also occurs because of a 'slow virus'[16,19]. It was later shown that the scrapie agent is highly resistant to ionizing and UV radiations[20–22]. A similar resistance was seen for the CJD agent[23]. These findings led to the conclusion that the agents causing these diseases possessed highly unusual properties.

The nature of the infectious agent was highly debated. Ideas regarding its nature ranged from it being a small DNA virus or a membrane fragment, to a polysaccharide or a protein[24–30]. It was observed that procedures that modified or hydrolysed proteins (such as treatment with sodium dodecyl sulphate (SDS), urea, guanidinium thiocyanate or phenol) affected the infectivity, whereas procedures that modified nucleic acids did not[10,31–33]. The results established, for the first time, that a protein was required or responsible for these unusual diseases. The infectious agent was named as prion ('proteinaceous infectious particle')[10].

After it was established that the infectious agent is a protein, efforts were directed towards discovering the identity and properties of this protein. It was observed that a purified sample, which was enriched in scrapie infectivity, contained mostly one protein[34,35], which showed remarkable resistance to protease cleavage. Resistance to proteinase K cleavage helped in the isolation of a protein fragment of an apparent molecular weight of 27–30 kDa, which was called PrP 27–30 (refs 36 and 37). The resistance to proteolysis hindered sequence determination of this protein[36]. However, sequencing of its N-terminal region led to the subsequent molecular cloning of the PrP gene[1,2]. It was realized that PrP 27–30 is the N-terminally truncated part (residues ~ 89–231) of the full-length prion protein[1,2].

Interestingly, PrP was detected at similar levels in crude lysates of scrapie-infected brain and in normal brain[37], supporting the hypothesis that PrP might be a secondary component involved in the disease[38]. It was, however, seen that the structural properties of the protein were different in the uninfected and diseased animals, which suggested that the normal (cellular) form of the prion protein (PrP^{C}) adopts an alternative conformation (PrP^{Sc}) in prion diseases[39].

There has been much debate about whether prion diseases occur through the novel alternative conformation of the protein, or not. Evidence supporting the 'protein only hypothesis' is that the prion protein is required for pathogenesis, as mice lacking the prion protein never develop prion diseases[40,41]. It has also been observed that overexpression of the prion protein causes a decrease in the incubation period (the duration between infection and appearance of disease symptoms) of prion diseases, as well as an increase in susceptibility, suggesting that the protein is important for prion pathogenesis[42]. Furthermore, in the presence of lipid and RNA, full length recombinant moPrP converts *in vitro* into an infectious isoform[43]. Upon intra-cerebral injection into mice expressing the normal level of prion protein, they develop disease with all the neuropathological hallmarks of prion diseases[43]. These observations confirm that no genetic material is required for prion transmission. The conversion of PrP^{C} into its pathogenic isoform is facilitated by RNA (polyanions) and lipid, which can also be achieved just by changing the physical nature of the reaction conditions[44].

The PrP^{Sc} conformation and prion-mediated toxicity

The nature of PrP^{Sc} is still poorly defined, but it forms an aggregate, which shares features of amyloid fibrils formed by many other proteins. Amyloid fibrils are protein aggregates with a high internal order. They possess a characteristic cross-β motif, a β-sheet bilayer, in which the sheet is organized parallel to and the β-strands perpendicular to the fibril axis[45,46]. The formation of amyloid fibrils by specific proteins is associated with specific neurodegenerative disorders[47,48]. Like amyloid fibrils, the PrP^{Sc} conformation of the prion protein is β-rich[49], and is thermodynamically more stable[50], more resistant against protease digestion[34–37] and less soluble than its normal cellular counterpart, PrP^{C}. Furthermore, prion rods, seen during the purification of PrP^{Sc} from the diseased brain, display properties of amyloid fibrils[51]. The amyloid plaques, formed in prion diseases, are rich in prion protein[52–54]. Thus, it seems that PrP^{Sc} represents either amyloid fibrils of the prion protein, or amyloid aggregates formed during the course of amyloid fibril formation by the prion protein.

Although the formation of PrP^{Sc} is often associated with prion diseases, the molecular mechanism of prion-mediated toxicity is unclear. Mice lacking PrP^{C} are normal, and resistant to prion disorders[40,41], suggesting that the loss of PrP^{C} function due to its conversion into PrP^{Sc} is not the cause of the disease. Grafting PrP^{Sc} into a brain region lacking PrP^{C} does not lead to prion pathogenesis[55], suggesting that PrP^{Sc} is not toxic by itself. More recently, it was shown that depleting PrP^{C} prevents disease and reverses spongiosis[56,57], suggesting that there is a constant requirement of PrP^{C} for pathogenesis. Furthermore, prion pathogenesis does not show a correlation with the amount of PrP^{Sc} and sometimes the disease occurs even in the absence of any detectable PrP^{Sc}, suggesting again that PrP^{Sc} may not be the toxic form[58–63].

In the case of amyloid-related diseases, a view has emerged that the final amyloid fibrils are not the toxic form. Instead, the intermediate oligomers and protofibrils formed along the pathway of fibrillation appear to be the toxic forms[48,64–66]. Along similar lines, it is possible that during the process of conversion of PrP^{C} to PrP^{Sc},

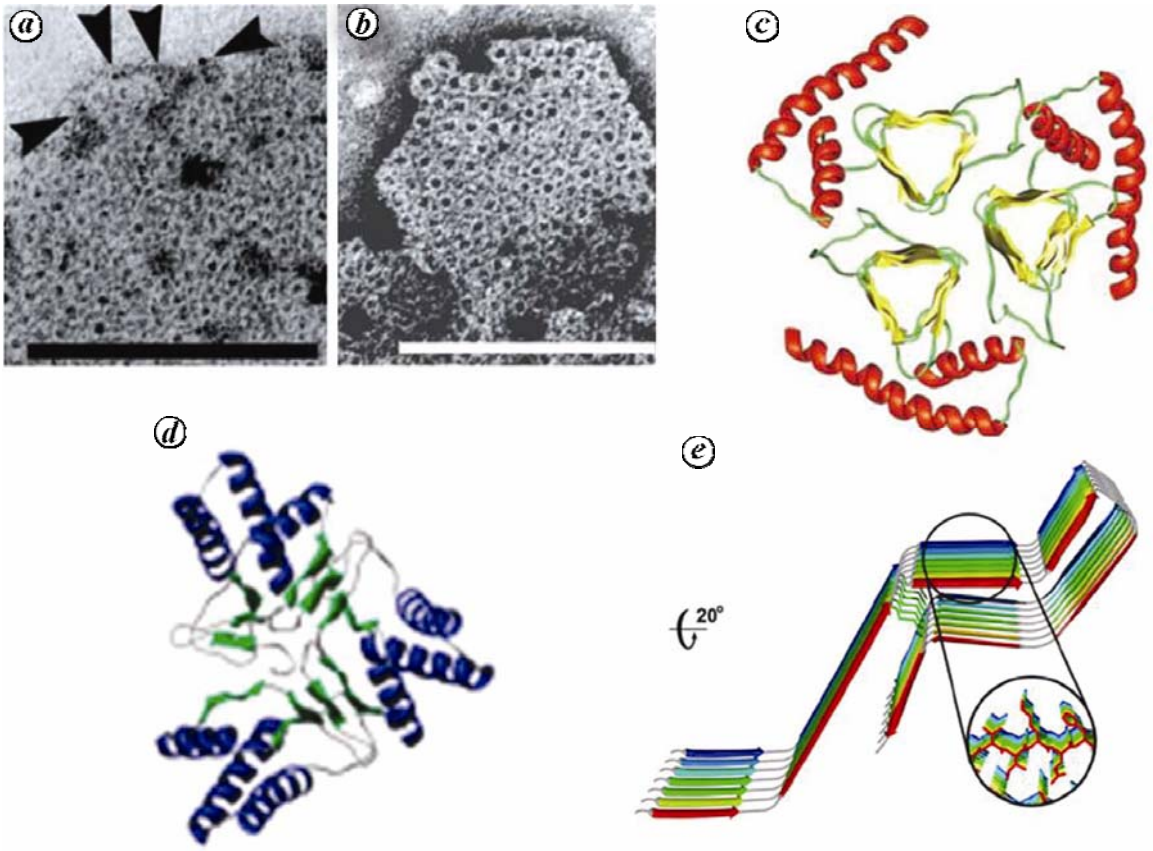

Figure 2. Structural models of prion aggregates. ***a***, Uranyl acetate-stained two-dimensional crystals of nanogold-labelled PrP 27–30. The high contrast of the uranyl stain has obscured some of the labels. However, a few are clearly visible (arrowheads). Reprinted with permission from Wille *et al.*[74]. ***b***, Two-dimensional crystals of PrP 106, stained with uranyl acetate. The scale bars in panels (***a***) and (***b***) represent 100 nm. Reprinted with permission from Wille *et al.*[74]. ***c***, A top-down view of the left-handed β-helical model (reprinted with permission from Govaerts *et al.*[75]). ***d***, The spiral model of protease-resistant PrP. Reprinted with permission from DeMacro and Daggett[76]. ***e***, Parallel in-register structure of the amyloid fibrils formed by the C-terminal domain of PrP. Reprinted with permission from Cobb *et al.*[82].

intermediate oligomeric states, which are toxic, accumulate. Indeed, it has been reported that an oligomer is the most infectious species in prion disorders[67]. The oligomeric forms found at the initial times of prion aggregation appear to be toxic[68]. But mature amyloid fibrils formed by the prion protein have also been reported to show toxicity[68], as do mature fibrils formed by other proteins[69]. It seems that fibril fragmentation enhances the cytotoxicity associated with amyloid fibrils[69], but it remains to be seen whether fibril fragmentation increases the amount of toxic oligomeric intermediates of the prion protein as well as of other amyloidogenic proteins.

Structural studies on PrP^{Sc}-like conformations and regions involved in PrP^{C} to PrP^{Sc} transition

While a high-resolution structure of PrP^{C} is available[70], not only is the structure of PrP^{Sc} ill-defined, but so also is its size, because of its high heterogeneity and insolubility. No covalent modification has been shown to be required for PrP^{Sc} formation[71,72]. Fourier-transform infrared (FTIR) spectroscopy of PrP^{Sc} shows a β-rich structure[49]; in contrast, PrP^{C} is α-rich. Epitope mapping also shows that PrP^{C} and PrP^{Sc} have different structures[73]. Furthermore, PrP^{Sc} has higher thermodynamic stability[50], and, as noted above, a greater resistance to protease digestion[34–37].

Multiple models have been proposed for the structure of PrP^{Sc}. Electron crystallography of the two-dimensional crystals of PrP 27–30 (described above; Figure 2 *a*) and a mini-prion, PrP^{Sc}106 (Δ23–88, Δ141–176; Figure 2 *b*)[74] has suggested a model (Figure 2 *c*) in which residues 89–175 form left-handed β-helices and the C-terminal region remains in the native-like conformation[75].

Some molecular dynamic simulation studies have suggested that the core of amyloid protofibrils of the prion protein is composed of three-stranded sheets containing residues 116–119, 119–132 and 160–164 and an isolated strand containing residues 135–140 (ref. 76). The growth of protofibrils appears to occur via association of identical interfaces in which the isolated fourth strand is connected

to the three-stranded sheet forming a continuous four-stranded sheet, where the first and fourth strand interface forms spiral protofibrils with a 3_1 axis of symmetry (spiral model; Figure 2 *d*). According to this model, the three helices of the native protein are mostly unaffected or intact in protofibrils[76]. This model was also found to be consistent with the 2D crystal of PrP^{Sc} (Figure 2 *a*). An experimental assessment of the β-helical and spiral model has suggested that the spiral model for PrP^{Sc} (Figure 2 *d*) is consistent with most of the biochemical characteristics of the PrP^{Sc} conformation[77]. An important result of these studies is that the α-helices of the C-terminal domain retain their structure, and do not participate in the conversion of PrP^{C} to PrP^{Sc}.

On the other hand, a comparison of several features of the structure of PrP^{C} to structures in a databank of 'normal' proteins has suggested that the most unusual structural features of PrP^{C} are found in helix 2 (residues 172–194), which appears to be energetically frustrated in its helical state[78]. Molecular dynamics simulations suggest that the second half of helix 2 (residues 184–194) and parts of helix 3 (residues 200–204 and 215–223) undergo a transition from an α-helical conformation to a β and/or random coil state during PrP^{C} to PrP^{Sc} conversion[79]. These results are consistent with recent hydrogen exchange (HX), electron paramagnetic resonance (EPR) spectroscopy, and solid-state NMR (ssNMR) studies (see below).

The structure of amyloid fibrils formed by recombinant human prion protein (r-huPrP) has been studied in detail. They are formed at pH 7, typically in the presence of 2M guanidine hydrochloride (GdnHCl), and are shown to be infectious in transgenic mouse models over-expressing PrP^{C} (ref. 80). HX, site-directed spin labelling and EPR spectroscopy have suggested that the core of r-huPrP amyloid fibrils is composed of the C-terminal region of the protein molecule, which spans helix 2, a major part of helix 3, and the loop between these two helices in the native structure[81,82]. No extensive hydrogen bonding, as indicated by the lack of significant protection against HX of amide hydrogens, has been detected in the N-terminal part of the PrP 90–231 fibrils, arguing against the involvement of the N-terminal region in the β-structure core. Single line spectra observed in the core region of PrP using site-directed spin labelling and EPR spectroscopy have suggested that these residues form monolayers that stack on top of one another, forming a parallel in-register β-structure (Figure 2 *e*)[82]. ssNMR studies of the full length Syrian hamster PrP (shaPrP; 23–231 residues) amyloid fibril, also suggest that the core of mammalian prion amyloid fibrils corresponds to residues 173–224 (ref. 83), and that the β-sheets are indeed arranged in a parallel in-register structure (Figure 2 *e*). Hence, high-resolution data strongly indicate that the PrP^{C} to PrP^{Sc} conformational transition occurs in the C-terminal domain during amyloid fibrillation.

The amyloid fibrils formed by many other proteins too, including amyloid β[84,85], α-synuclein[86], tau[87], barstar[88] and yeast PrP (Sup35NM, Ure2, Rnq1)[89–91] adopt in-register parallel β-sheet conformations, in which the adjacent peptide chains line up in the same N to C orientation, with corresponding residues apposing each other. It seems to be the most common fold of amyloid fibrils.

The Y145 stop mutation in huPrP (huPrP 23–144) is associated with inherited prion disorders. There have been extensive structural studies of the amyloidogenic aggregates of this protein variant. Magic angle ssNMR spectroscopy has suggested that the core of the amyloid fibrils formed by this variant encompasses residues 112–141 (ref. 92), and that most of the other residues are largely disordered. The core is composed mainly of three β-strands, containing residues 112–115, 118–122 and 130–139. Similarly, a study with a moPrP 89–143 variant, containing the inherited prion disorder-associated mutation P101L, has suggested that residues 112–124 adopt an extended β-sheet conformation[93]. HX measurements have suggested that the core of fibrils formed by this fragment is composed of two β strands, containing residues 102–109 and 117–136, joined by a conformationally heterogeneous turn formed by residues 110–116 (ref. 94). From these studies, it seems that in the case of prion fragments lacking the C-terminal domain, the fibrillar core is composed mostly of residues 102–139. But in the case of the full-length prion protein, residues 160–220 form the core of the fibrils, and it remains to be answered as to why, despite their propensity to adopt a β-sheet conformation, residues 102–139 do not participate in fibrillation of the full-length protein.

The structure of infectious PrP^{Sc} remains obscure. ssNMR-based studies have been carried out on an infectious sample of yeast PrP[91,95], but it is possible that in these studies the physical properties of the bulk of the amyloid do not represent those of the minority of the infectious amyloids. The structure of an infectious sample of mammalian rPrP has also been determined[80–82,94,96], but the infectivity of this sample was quite low. Importantly, it is now possible to generate infectious PrP^{Sc}-like conformations, whose infectivity is similar to that of PrP^{Sc} isolated from animals, from rPrP *in vitro*. This would certainly be of great help in understanding the structural features of infectious PrP^{Sc}. A recent HX study with infectious PrP^{Sc} has revealed that the core is composed of residues 80–90 to 231 (ref. 97).

While understanding the structures of amyloid fibrils and infectious PrP^{Sc} is important, one also needs to understand how they form. Also, it is necessary to know how the aggregation process gets initiated, what kinds of intermediates are formed, and the kinds of residues and interactions that are important for their formation. Not only will these studies lead to a better elucidation of the features of prion diseases, but will also help in the generation of therapeutics.

Mechanism of amyloid fibril formation

Amyloid fibril formation seems to commence from partially structured conformations of proteins[98–100], which appear to provide the necessary intermolecular interactions for assembly. But owing to their transient nature, direct structural information on aggregation-competent, partially unfolded conformations is available only for a few proteins[101,102]. Partial unfolding in the case of a globular protein and partial folding in the case of a natively unfolded protein, both leading to the formation of an aggregation-competent, partially-structured conformation, can be induced by mutations, by changes in the environmental conditions or upon chemical modification[103]. Although a structural perturbation of the native structure resulting in the formation of a partially structured conformation seems to be necessary, a globular protein could conceivably expose a locally unfolded segment, for example, during its conformational breathing motions, to form amyloid fibrils[104].

The mechanism of protein aggregation is often describable by two basic models, nucleation-dependent polymerization (NDP) and isodesmic (linear) polymerization[105–109]. An NDP reaction consists of two stages, nucleation and growth. The nucleation phase consists of a number of thermodynamically unfavourable equilibria. The nucleus represents the highest energy structure, and its formation constitutes a bottleneck in the polymerization reaction. Once the nucleus is formed, subsequent steps become favourable. The kinetics of an NDP reaction[107,108] shows a lag phase, which is abolished when a small amount of nucleus in the form of fully formed fibril is provided as a seed at the beginning of the reaction. There is a critical concentration for the formation of a polymer, and a strong dependence of the nucleation rate on protein concentration. On the other hand, an isodesmic (linear) polymerization reaction[106] does not involve separate nucleation and elongation phases, and polymerization from any of the monomeric subunits is equally favourable[110,111]. Each association step involves an identical interaction; consequently, the rate constants are independent of polymer size. Thus, an isodesmic polymerization reaction resembles the elongation phase of an NDP reaction. The kinetics of an isodesmic polymerization reaction does not involve a lag phase, and no critical concentration exists.

Kinetic studies can distinguish between the two polymerization models, but it is not easy to do so because the distinction between them is not always robust, and depends on the nucleus size as well as on the association and dissociation rate constants. Furthermore, NDP and isodesmic models represent two extremes of protein polymerization, and it is conceivable, as seen for amyloid fibril formation by several proteins, that a polymerization reaction can possess features of both models[109,111].

For a few proteins, the amyloid fibrillation reaction can be described well as a NDP reaction. For the aggregation reaction of most proteins, however, the kinetics shows only weak dependences on protein concentration[112–116]. This weak dependence on protein concentration has been interpreted as an NDP mechanism involving a small nucleus size. A monomeric nucleus has been suggested in the case of polyQ peptides, which indicates that an unfavourable conformational change in the monomeric protein may constitute the rate-determining nucleation event[115,117]. An NDP mechanism with a monomeric nucleus would be similar to the monomer-directed conversion model, a model proposed for PrP^{C} to PrP^{Sc} conversion (see below). Furthermore, secondary nucleation events, such as nucleation on the surface of pre-existing fibrils or on exogenous impurities, have been proposed to occur during the formation of amyloid fibrils by a few proteins[108,112–114,116,118–120].

For many proteins, spherical oligomers and/or protofibrils are seen to form rapidly at the beginning of the aggregation reaction leading to the formation of mature amyloid fibrils. For such proteins, the aggregation mechanism has been referred to as 'assembly via oligomeric intermediates'[112,121–123]. In this mechanism, the formation of the pre-fibrillar aggregates appears not to be limited by an unfavourable nucleation event, and, therefore, can be considered as isodesmic polymerization. Because of the heterogeneity inherent in the process, and the insoluble nature of mature fibrils, it is not easy to carry out kinetic measurements to determine whether the pre-fibrillar aggregates are on the direct pathway to mature fibrils, or whether they are off-pathway aggregates. For example, in the case of yeast prion protein Sup35NM, single molecule experiments indicate that fibril growth occurs by monomer addition[113], which would suggest an off-pathway role for the pre-fibrillar aggregates that have been reported in other studies[112] to be on-pathway. Nevertheless, for some proteins, it appears that the pre-fibrillar aggregates do lie on the direct pathway of fibril formation[124–129]. In such cases, amyloid fibril formation might nucleate within the pre-fibrillar aggregates and grow via many different ways[109].

In most amyloid fibril formation reactions, the growth of aggregates and the acquisition of β-sheet structure seem to be coupled[112,121,128,130–132]. It appears that the associating units (monomers or oligomers) first add on to the ends of the growing aggregates, and then undergo the β-sheet conformational change. Recently, it has been seen for three proteins that amyloid fibril formation occurs from conformationally converted oligomeric intermediates, i.e. the β-sheet conformational change occurs in the oligomeric intermediates before they associate with the ends of growing aggregates[123,127,133].

It seems that any individual protein can adopt multiple, distinct fibrillar morphologies[134], and that a range of pre-fibrillar states precedes the formation of fibrils by many

proteins. In the case of the prion protein, it appears that structural heterogeneity prevails at the level of prefibrillar oligomers and protofibrils[133]. In this context, an understanding of the initial and intermediate stages of amyloid fibril formation reactions can provide an insight into the structural heterogeneity inherent in mature fibrils. Understanding the structural as well as the kinetic basis of the conformational polymorphism seen in amyloid fibril structures is a major goal of studies on protein aggregation, including prion protein aggregation studies. Prion diseases have several characteristic features not shared by other neurodegenerative diseases associated with amyloid fibril formation, and it is crucial to gain molecular-level insight into how these features arise.

Characteristic features of prion diseases

Infectiousness

The PrP^{Sc} conformations can replicate themselves and cause the conversion of PrP^{C} to its PrP^{Sc} self[10,11]. The ability to be infectious in this manner differentiates prion diseases from other amyloidogenic disorders. Prion replication is often described either by a refolding model (monomer-directed conversion; Figure 3 *a*) or by a seeding model (nucleation-dependent polymerization; Figure 3 *b*). According to the refolding model[135], PrP^{C} and PrP^{Sc} are separated by a high activation energy barrier, and the conformational change associated with PrP^{C} to PrP^{Sc} conversion constitutes the rate-limiting step for the process.

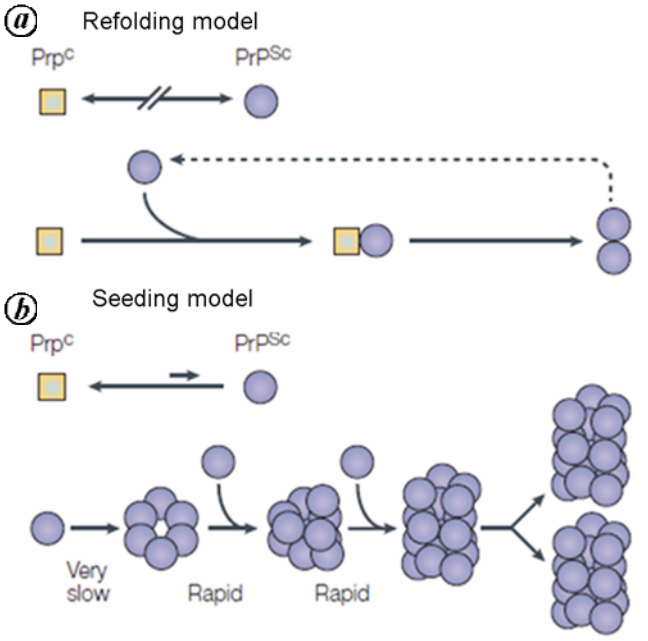

Figure 3. Models for the conversion of PrP^{C} to PrP^{Sc} (an alternative conformation). Yellow squares represent PrP^{C} and blue circles PrP^{Sc}. ***a***, Refolding model and ***b***, Seeding model. Reprinted with permission from Weissmann[137].

PrP^{Sc} acts as a template and upon interaction induces a conformational change in PrP^{C} to convert it into PrP^{Sc}. According to the seeding model[136], PrP^{Sc} exist as oligomers, whose formation from PrP^{C} involves a number of unfavourable equilibria. PrP^{Sc} is therefore regarded as the nucleus of a classical nucleation-dependent polymerization reaction (see below). Upon formation, PrP^{Sc} acts as a seed to convert more PrP^{C} into PrP^{Sc}, leading to the formation of prion fibrils. Because of the presence of an unfavourable nucleation step, there is a lag phase in the reaction. The exponential nature of the kinetics of this reaction suggests that the prion aggregates undergo continuous fragmentation to generate more and more seeds for growth[137]. Since PrP^{Sc} formation is always seen to be associated with oligomerization[67], the seeding model has been widely accepted as the more plausible mechanism for the replication of PrP^{Sc}. Both models of PrP^{Sc} formation (Figure 3) can be, however, described as slight variations of the NDP model, where the nucleus is monomeric in the case of the refolding model and oligomeric in the case of the seeding model.

Prion strains

The same prion protein can give rise to a range of infectious conformations (prion strains), which differ in their incubation periods, the brain area they affect, and their disease phenotypes[138–143]. Earlier, it was debated whether prion diseases occur because of viruses or proteins (see above). At that time, the observation of different prion strains led to opposition of the 'protein only hypothesis', because it was difficult to understand as to how a protein could adopt multiple conformations. Later, it was shown that the prion strains represent distinct conformations of PrP^{Sc}. These strains show differences in their protease digestion patterns[144], secondary structure content[145], epitope exposure[146], as well as stability towards thermal denaturation[147]. When different strains are transmitted to isogenic animals, strain differences become apparent as differences in incubation periods or phenotypes, suggesting that differences in strains are not because of differences in the hosts[148], but arise from differences in the structure of PrP. Strains also appear to differ in glycosylation patterns, and in the attachment of GPI anchors[149,150]. The role of these covalent changes versus non-covalent structural changes, in defining the strain is, however, not understood[143,151].

Species barrier

Infectious prion isolated from one species either does not transmit or transmits with a longer incubation period, into another species. This phenomenon is referred to as the 'species barrier' for prion transmission[24]. In the case where transmission of prion from one species to another occurs

with a longer incubation period, subsequent transmission to the same species occurs with a decreased incubation period. After many rounds of transmission in the same species, the incubation period becomes fixed[24]. This phenomenon is known as adaptation.

It now appears that many of the characteristic features of prion diseases may originate from the amyloid formation reaction of the prion protein. It is important to critically examine the mechanism of mammalian prion protein aggregation, the structural heterogeneity inherent in the process, as well as the possible roles prion aggregation may play in determining the characteristic features of prion diseases.

Recombinant PrP as a model system to study prion aggregation

Recombinant prion protein (rPrP) has been used extensively to study the aggregation of prion proteins. Like naturally occurring PrP, rPrP has a folded C-terminal domain and an unstructured N-terminal domain, and has the disulphide bond linking helices 2 and 3 intact. Although it lacks any post-translational modifications, including the C-terminal GPI anchor, its structure and thermal stability are similar to those of naturally occurring PrP[152]. This suggests that post-translational modifications do not affect significantly the stability and structure of PrP^{C}. Furthermore, as mentioned earlier, it can be converted *in vitro* into an infectious prion isoform[43,44]. Thus, it becomes an easily producible and useful model system to study the conversion of PrP^{C} into PrP^{Sc}.

Mechanism of amyloid fibril formation by the prion protein

Onset of prion aggregation

The observation that amyloid fibrillation reactions commence from partially structured conformations (see above) suggests that the process of fibril formation is linked intricately with the folding reaction. There have been several studies of the folding of the prion protein, mostly with fragments (PrP 90–231 or 121–231) containing the C-terminal domain, which has a folded structure. The prion protein folds rapidly; hence it has been difficult to study its folding kinetics and to characterize its folding pathway. Early stopped-flow mixing studies of the folding and unfolding of the C-terminal prion domain 121–231 had suggested that this domain folds without any detectable intermediate[153]. Later studies showed the presence of a folding intermediate, as suggested by the deviation from linearity in the folding arm of the chevron plot, and a burst-phase change in fluorescence during the reaction[154]. The folding intermediate was found to be populated more at acidic pH than at neutral pH[154]. Continuous-flow mixing measurements showed that there are two distinct phases in the folding reaction of the rhuPrP 90–231 (ref. 155), providing direct evidence for the rapid accumulation of an early folding intermediate (with a time constant of 50 μs), followed by a rate-limiting folding step (with a time constant of 700 μs)[155]. The presence of a folding intermediate has also been shown by HX studies in native-like conditions[156]. A high-pressure 2D NMR study has suggested the presence of a metastable unfolding intermediate at pH 5.2 (ref. 157).

It has been suggested that an alternative conformation of the prion protein (PrP*) binds to PrP^{Sc} and gets converted into PrP^{Sc} conformation[158,159]. The aggregation rate shows no direct correlation either with the destabilization of the native prion protein or with the familial mutations associated with the prion diseases[160]. Interestingly, the familial mutations associated with prion diseases appear to stabilize the folding intermediate[161], suggesting that PrP^{Sc} formation might be commencing through this folding intermediate. Moderate concentrations of denaturants stabilize the folding intermediate and facilitate aggregation[154,162]. The observation that the intermediate present in the folding or unfolding pathway of the prion protein is populated more at acidic pH is consistent with the view that PrP^{Sc} formation can occur in the endocytic pathway where the pH is slightly acidic[163,164].

These indirect lines of evidence suggest that the aggregation of PrP may initiate from the monomeric folding or unfolding intermediate. Direct kinetic evidence correlating the amount of intermediate, when modulated either by denaturant concentration or by mutation, with the rate of aggregation, is yet to be obtained.

Equilibrium between α-rich monomer and β-rich oligomer

Native PrP, which is rich in α-helical structure, undergoes a structural transition into a β-rich conformation in the presence of a trace amount of urea with NaCl, or of GdnHCl[162,165–167]. The β-rich conformation has exposed hydrophobic surfaces, as indicated by increased ANS binding[165], and is oligomeric. Its formation involves concurrent protein–protein association and conformational change[166]. The β-rich oligomer appears predominantly octameric, as suggested by electrospray mass spectrometry measurements[168]. The native disulphide bond remains intact during the oligomerization process[166]. The observation that a partially denaturing condition and acidic pH accelerate conversion into β-sheet suggests that the unfolding intermediate might be involved in the formation of the β-rich oligomer.

The pH-dependence of the structural transition suggests that the α-rich monomeric PrP exists in equilibrium with the β-rich oligomer[168–170]. The equilibrium favours

the α-rich monomeric PrP at neutral pH, and the β-rich oligomer at acidic pH. The β-rich oligomer appears to be separated from the α-rich monomeric PrP by a large activation energetic barrier[167]. The kinetics of the structural transition of the α-rich monomeric PrP into β-rich oligomer is hyperbolic, as monitored by the change in the secondary structure as well as by the increase in size, using size exclusion chromatography[166]. The reaction does not show any effect of seeding, suggesting that this process is not autocatalytic, which is characteristic of PrP^{C} to PrP^{Sc} conversion (see above).

Recently, β-rich oligomers have been seen to form at pH 2, in the absence of any denaturant[128,129,133]. At this pH, their structure appears to be different from those of other β-oligomers reported earlier. Prion oligomers rich in β-structures are also formed upon removal of the disulphide bond in the presence of NaCl[171,172]. Furthermore, discrete soluble oligomeric forms are seen to form upon thermal unfolding of the prion proteins at low pH ($\sim$ 3.5) in the presence of salt[173–175].

Although the far-UV CD spectra of the oligomers formed in different conditions suggest that they are β-rich, they differ in their FTIR spectra[173–175]. It therefore appears that high structural heterogeneity exists in the oligomeric aggregates formed by the prion protein. In order to understand the phenomenon of prion strains, it is crucial to determine the role of structurally distinct prion oligomers in the amyloid fibril formation reaction, as well as in the pathological diversity of the prion proteins.

Transition of α-rich monomer into amyloid fibrils

The α-rich monomer, the predominant form present at neutral pH, forms long, straight amyloid fibrils in the presence of a denaturant, in a process that appears to be nucleation-dependent (pathway I; Figure 4 *a* and *b* and 5)[114,168–170]. The aggregation kinetics involves a lag phase (Figure 4 *b*), which is abolished upon the addition of a small amount of seed at the beginning of the reaction. However, the aggregation properties of the prion protein are not completely consistent with the classical NDP model (see above). Although the kinetics involves an initial lag phase, the lag phase is only weakly dependent on protein concentration, and does not fit to a t^2 dependence[114] (Jain and Udgaonkar, unpublished). This suggests that the aggregation reaction involves secondary nucleation events[114]. A plot of the log of the elongation rate versus the log of the protein concentration was seen to be linear, with a slope of 1, suggesting that the rate-limiting step of polymerization is conformational rearrangement in the polypeptide upon assembly, rather than association[114].

The length of fibrils depends on pH[114]; shorter fibrils form near neutral pH, where fibrillation is faster, and longer fibrils form at lower pH, where the fibrillation kinetics is slower. This observation has been interpreted in terms of the off-pathway nature of the β-rich oligomer. Near neutral pH, a higher amount of monomers leads to rapid nucleation. Hence a large number of nuclei are formed, leaving behind a small concentration of monomers available for elongation, and, consequently, shorter fibrils are formed. At acidic pH, the equilibrium shifts in favour of the β-rich oligomer, and due to a smaller concentration of the α-rich monomer, fewer nucleation sites are formed, leaving behind a relatively larger concentration of monomers to take part in the elongation of the nuclei into fibrils. Consequently, longer fibrils are formed at acidic pH.

In a recent study (Figure 6), spherical oligomers were seen to form during the initial lag phase of the kinetics of amyloid fibril formation at neutral pH. Interestingly, these oligomers appear to be capable of seeding the aggregation reaction, which suggests that they are on the direct pathway to the mature fibrils (Jain and Udgaonkar, unpublished). The presence of an oligomeric intermediate can explain the unusual nature (weak dependence of the lag phase as well as of the aggregation rate constant on protein concentration) of prion protein aggregation (see above). It would be important to characterize the core of these oligomers and fibrils in order to gain insights into how these oligomers lead to the formation of fibrils.

High-resolution atomic force microscopy studies on the long, straight amyloid fibrils formed by the full-length mouse prion protein (moPrP) have suggested that the fibrils are highly heterogeneous in their structures. They differ in the number of protofilaments as well as in the manner in which the protofilaments are intertwined to form fibrils[176]. Several other studies have also exposed the heterogeneity inherent in prion fibril structures. Changes in the aggregation conditions have been seen to lead to the formation of morphologically distinct prion fibrils which differ in their stabilities, as monitored by epitope exposure using ELISA at different GdnHCl concentrations[177]. Differences in shaking conditions were also found to lead to structurally and morphologically distinct fibrils (S-shaped and R-shaped fibrils)[178], but it seems that a contamination of 0.1–1% PrP 30–231 in the full-length PrP 23–231 preparation was responsible for these two conformational variants of fibrils[179]. These two fibril polymorphs had different folding patterns of the β-strands, as characterized by CD, FTIR, HX, proteinase K digestion and the binding of conformation-sensitive fluorescence dyes, suggesting that they had different secondary, tertiary and quaternary structures[180].

The β-rich oligomer leads to the formation of worm-like fibrils

Many studies had suggested that the β-rich oligomer is an off-pathway aggregate and does not directly participate in

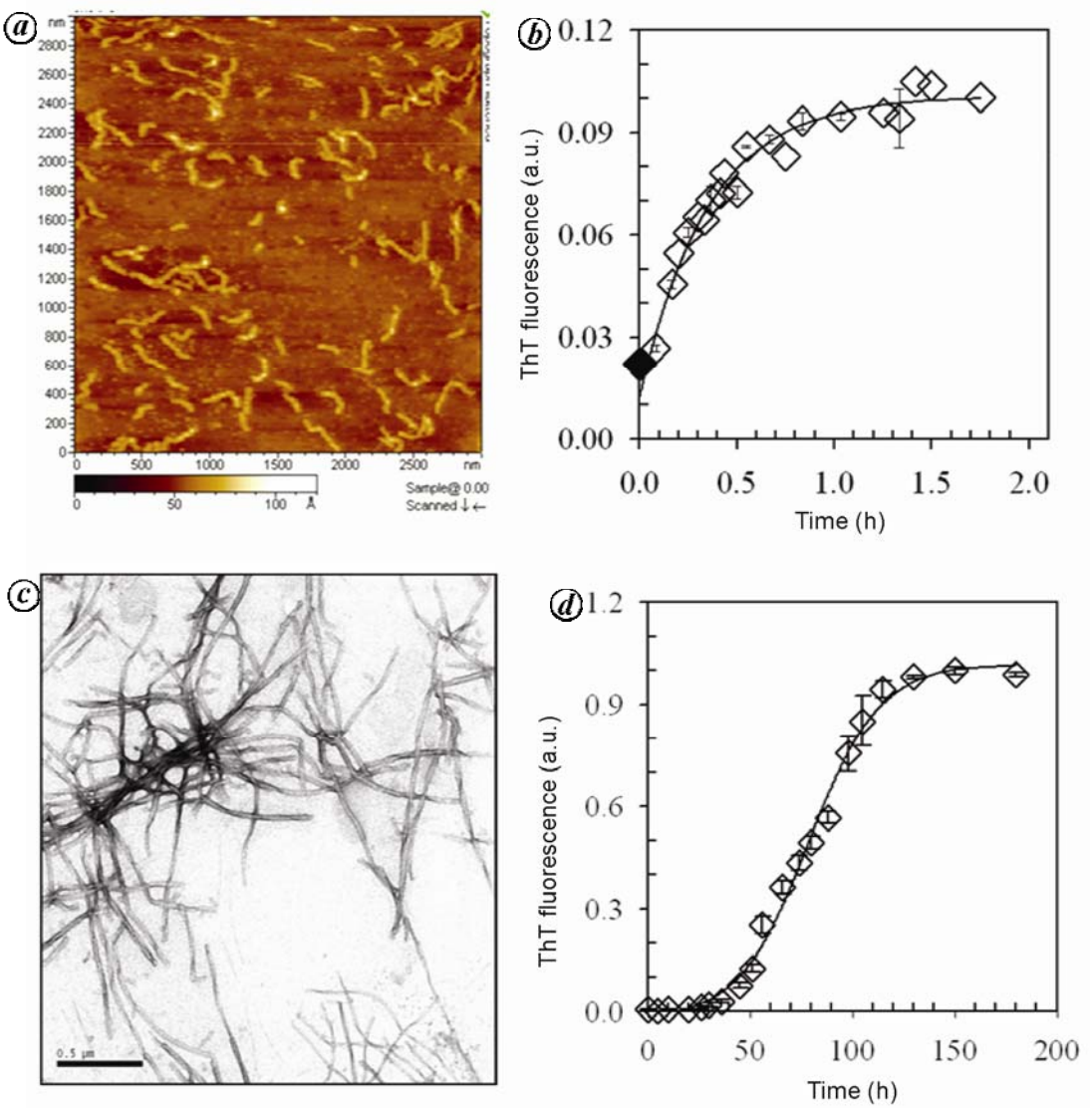

Figure 4. Amyloid fibril formation by the mouse prion protein. ***a***, AFM image of worm-like fibrils formed at pH 2. ***b***, Kinetics trace of worm-like fibril formation at pH 2. ***c***, EM image of long, straight fibrils formed at pH 7. ***d***, Kinetic trace of long, straight fibril formation at pH 7.

the aggregation reaction leading to the formation of long straight fibrils by the prion protein. An off-pathway role for the β-rich oligomer had been indicated by a study of the pH dependence of the formation of long, straight fibrils (see above), which showed that the length of the lag phase decreases with an increase in the amount of the α-rich monomer, and increases with an increase in the amount of the β-rich oligomer. This suggested that the formation of long, straight fibrils commences from the α-rich monomer[169]. Epitope mapping, proteinase K digestion and peptide mapping suggested that the β-rich oligomer and long, straight amyloid fibrils have different internal structures[168]. The off-pathway nature of the β-rich oligomer is consistent with the dependence of the length of the long, straight fibrils on the pH of the reaction (see above).

It is important to realize that the studies suggesting an off-pathway role for the β-rich oligomer involved the use of high concentrations of salts and denaturant[168–170], which can inhibit the growth of the β-rich oligomer. In the presence of a low concentration of salt and in the absence of denaturant, the β-rich oligomer, formed by moPrP gives rise to worm-like fibrils at pH 2 (Figure 4 *c* and *d*)[128,133], having a fibrillar morphology that is structurally different from that of the long straight fibrils formed from the α-rich monomer (pathways II and III; Figures 4 *a*, *c* and Figure 5). The worm-like fibrils have smaller diameters, as determined from their heights on AFM mica, and curly morphologies (Figure 4 *c*). Interestingly, worm-like fibril formation involves a pathway that is distinct from that of the long, straight fibril formation. The kinetics of worm-like fibril formation is hyperbolic;

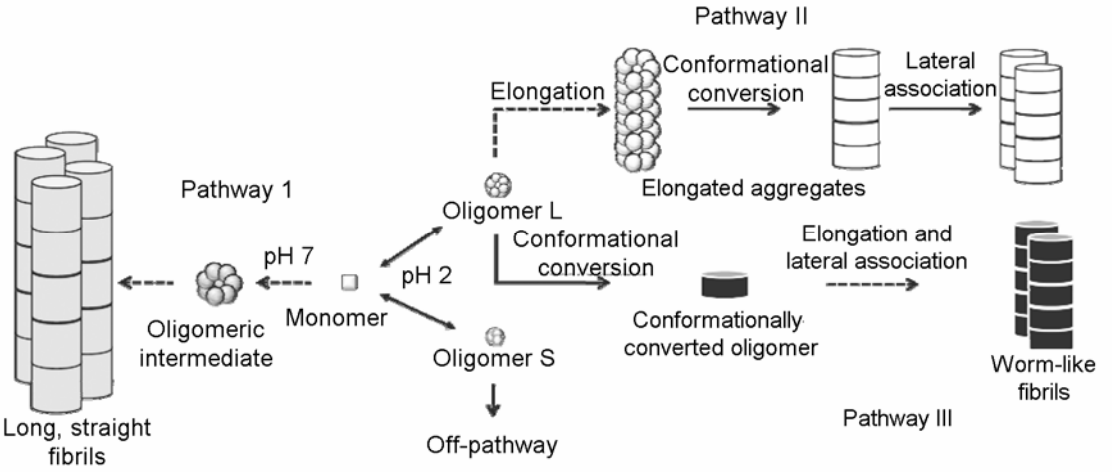

Figure 5. Pathways of amyloid fibril formation by the prion protein. The α-rich monomeric form of the prion protein exists in a pH-dependent equilibrium with the β-rich oligomer. At pH 7, the equilibrium favours the α-rich monomers, which, in the presence of sub-denaturing concentrations of denaturant and upon shaking at 37°C, form long, straight amyloid fibrils (pathway I). The transition of the α-rich monomer into long, straight fibrils occurs through spherical oligomeric intermediates, and the transition appears to be nucleation-dependent. The equilibrium between the α-rich monomer and the β-rich oligomer favours the latter at low pH. The β-rich oligomer converts into worm-like fibrils in a process that appears not to be limited by an unfavourable nucleation event. The β-rich oligomer consists of two distinct oligomeric sub-populations, the larger oligomer (oligomer L) and the smaller oligomer (oligomer S). Oligomer S appears to be an off-pathway aggregate formed in competition with the on-pathway oligomer L. The transition of oligomer L into worm-like fibrils occurs through alternative pathways. In one pathway (pathway II), which operates at 120 mM NaCl, the β-sheet conformational conversion follows aggregate growth, while in the other (pathway III), which operates at 200 mM NaCl, the β-sheet conformational conversion precedes aggregate growth. In pathway II, lateral association of the elongated aggregates, which leads to the formation of mature, worm-like fibrils, constitutes the final step. In contrast, lateral association and β-sheet conformational conversion occur simultaneously in pathway III. The worm-like amyloid fibrils formed in the alternative pathways differ in their structures.

no lag phase is seen (Figure 4 *d*). The kinetics shows a weak dependence on protein concentration, and there is no apparent critical concentration, suggesting that the process is not limited by nucleation. It appears, therefore, that the formation of worm-like fibrils follows the isodesmic (linear) polymerization mechanism. It remains to be investigated whether the morphologically distinct fibrils formed on the separate pathways involve the same or different core segments of the amino acid sequence.

The fibrillation of moPrP and β_2-microglobulin shows remarkable similarity[128,181]. For both the proteins, the formation of long, straight fibrils commences from monomers in a nucleation-dependent manner, whereas an oligomer forms worm-like fibrils in a process that appears not to be limited by an unfavourable nucleation event (Figure 5). The aggregation reaction can be switched between the two pathways by a change in aggregation conditions[181]. It remains to be seen whether the fibril formation reactions of other proteins also share this feature.

The β-rich oligomer has been shown to consist of two distinct sub-populations, namely a large oligomer (oligomer L) and a small oligomer (oligomer S), which differ not only in their sizes but also in their secondary structures[129]. Interestingly oligomer L, and not oligomer S, transforms directly into worm-like fibrils (Figure 5)[129]. The transformation of the β-rich oligomer into worm-like fibrils occurs in multiple steps[128], and via alternative pathways[133]. The worm-like fibrils formed on the alternative pathways differ in their external dimensions as well as in their internal structures[133]. The reaction can be switched between the alternative pathways by carrying out the reaction at different salt concentrations (pathways II and III; Figure 5). Salts appear to modulate the aggregation mechanism via a direct physical interaction with the protein[133].

Fibril formation by the full-length prion protein requires unusual and typically drastic environmental conditions. The formation of long, straight amyloid fibrils requires the presence of 1–2 M of GdnHCl, or both 1 M GdnHCl and 3 M urea, with 150 mM NaCl (refs 168, 170, 182), and invariably requires agitation of the solutions. It is now possible to aggregate a mutant variant, associated with an inherited prion disorder, at pH 4 in the absence of any denaturant, but continuous shaking is essential for the induction of aggregation reaction[183]. The formation of worm-like fibrils occurs only at low pH, although it does not require agitation. It would appear that protonation of critical residues leads to the formation of an amyloidogenic conformation by destabilization of the native structure. The formation of worm-like fibrils would occur at undetectable levels, and slowly, at pH 7, because the protonated amyloidogenic conformation would be present at very low concentration at this pH. The slowness of the aggregation of such protonated amyloidogenic conformations may be physiologically relevant, because the prion diseases are late-onset diseases[184].

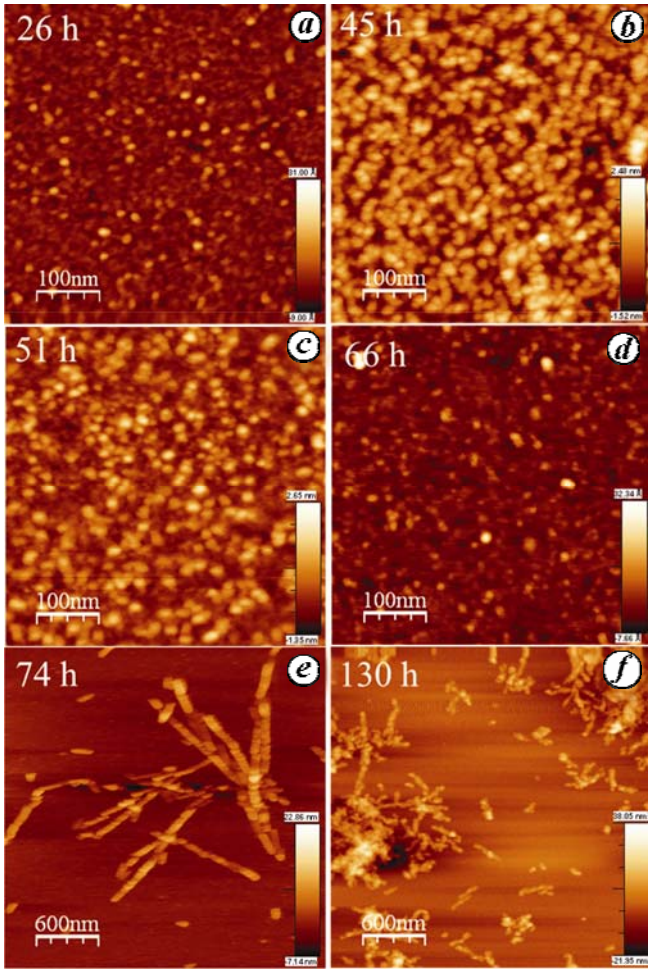

Figure 6. Progress of the aggregation reaction leading to the formation of long, straight fibrils. AFM images of aggregates formed at different time-points during the formation of long, straight fibrils by the mouse prion protein. The reaction was carried out at 37°C, pH 7, and with 750 rpm shaking. For the 26, 45 and 51 h time-points, the protein was diluted to 0.6 μM before applying onto the mica. In the case of the 66, 74 and 130 h time-points, the protein was diluted to 5 μM before applying onto the mica.

Molecular origin of the characteristic features of prion diseases

Infectiousness

The amyloid fibrils formed by yeast as well as by mammalian PrP adopt an in-register parallel β-sheet (see above). The parallel in-register structure can explain the infectious nature of prion proteins; the ends of the fibril provide a template guiding the conformation of the new monomer joining the fibril to be the same as the last monomer already in the fibril[185,186]. Presently, it is not known whether the conversion of PrP^{C} to PrP^{Sc} by PrP^{Sc} is similar to the conversion of the soluble proteins into amyloid fibrils by seeds from the fibrils.

Prion strain

The phenomenon of prion strain, wherein the same prion protein forms a range of infectious particles, appears to originate from the ability of a prion protein to aggregate into structurally distinct amyloid aggregates. Amyloid polymorphs of a prion protein may form by distinct arrangements of an amyloidogenic segment in different amyloid aggregates (packing polymorphism), by participation of different amyloidogenic segments in different amyloid aggregates (segmental polymorphism), or by a combination of the former two (combinatorial polymorphism)[187]. From the observation that distinct amyloid aggregates of prion can form *in vitro*, either upon protein mutation or upon a change in aggregation conditions, it is conceivable that different mutations in the prion protein, or fluctuations in the environmental conditions prevailing within cells, underlie the phenomenon of prion strains. It is insightful to consider the following observations.

Recently, it has been shown that prions can evolve in cell culture[188]. A heterogeneous population of brain-adapted prion, when transferred to cell culture, adapts to the cellular environment, and out-competes the original brain-adapted prion[188]. Upon re-inoculation into the brain, it is out-competed by the brain-adapted prion[188]. Similarly, in cell culture, a swainsonine inhibitor-resistant prion substrain becomes selected (evolved) in the presence of swainsonine inhibitor. The inhibitor-resistant prion substrain, in the absence of the inhibitor, is out-competed by an inhibitor-susceptible counterpart[188]. This suggests that the prion protein aggregates or PrP^{Sc} are highly heterogeneous and, depending on the environmental conditions, only a few conformations survive and are transmitted.

When amyloid polymorphs formed under different aggregation conditions, were inoculated into mice, it was observed that the stable amyloid fibrils produce a prion strain with a longer incubation period, whereas the more labile amyloid fibrils generated a different strain, which had a shorter incubation period[177]. As suggested by *in vitro* prion aggregation studies[176,178], these observations imply that the conformational inadaptability between various types of PrP^{Sc}, which appears to constitute the basis of prion strains and the species barrier, can originate also from the environmental conditions that they have evolved in.

Species barrier

The species barrier may originate from differences in the sequence of a few critical regions of the prion proteins from different species, which can lead to the formation of species-specific conformations of PrP^{Sc}. If the prion sequences of two species have differences in these critical regions, the PrP^{Sc} conformation of one would be incompatible with the prion sequence of the other, and the PrP^{Sc}

conformation of one would be incapable of converting the PrP^{C} of another species into PrP^{Sc}. It is instructive to consider the following observations[189,190].

PrP 23–144 has been used extensively as a model system to understand the species barrier as well as the strain phenomenon in prion diseases. Using different fragments, it was observed that the fragments ending before residue 139 did not show a propensity for amyloid fibrillation. This indicated that residues within the 138–141 segment are critical for amyloid fibrillation[191]. The PrP 23–144 fragments of huPrP, moPrP and shaPrP have distinct lag phases, and show differences in the structures of the amyloid fibrils formed. huPrP can be seeded with huPrP or moPrP, but not with shaPrP. moPrP can be seeded with either of the three, and shaPrP can be seeded only with shaPrP. A comparison of the amino acid sequences in the critical region 138–141 of the prion proteins from these three species shows species-specific differences at positions 138 and 139. Interestingly, species-specific substitutions of a single amino acid residue in the critical region can bypass the species barrier, as judged by seeding capability. Furthermore, the sequence-specific seeding specificity correlates well with the structural characteristics of the amyloid fibrils formed[189,190,192]. The degree of dissimilarity in the steric zipper structure seems to determine the transmission barrier[192]. Thus, it appears that amyloid fibrils of prion proteins of different species represent different strains, and that the species barrier, as well as prion strains, originate from the inability of the conformations of different prion sequences to adapt to each other in segments critical for amyloid fibril formation.

Conclusions

Studies with purified proteins are now providing insights into the mechanism of prion protein aggregation and the structures of prion aggregates. The aggregation reaction of the prion protein appears to commence from a partially structured conformation, and progression towards prion fibrils is highly dependent on the aggregation conditions. At neutral pH, the prion protein, under strongly destabilizing conditions, transforms into long, straight fibrils with sigmoidal kinetics, and the reaction appears to be nucleation-dependent. On the other hand, at acidic pH the prion protein aggregates, without any requirement of the presence of denaturant, to form worm-like fibrils, a fibril morphology that is strikingly different from that of the long, straight fibrils that form at neutral pH. The formation of worm-like fibrils follows hyperbolic kinetics and appears not be limited by an unfavourable nucleation event. Under both conditions, a structurally diverse ensemble of oligomeric species is populated at the initial stages of the reaction, which appears to lead to structurally distinct amyloid fibrils. The observation that structural heterogeneity exists also at the initial stages of fibrillation, suggests that it sets in early during the reaction. The formation of structurally diverse aggregates at the initial stages of the reaction suggests that many different precursor states could be utilized for the formation of mature prion fibrils. The transitions of distinct precursor states into prion fibrils appear to utilize distinct pathways of aggregation. A change in protein sequence or a change in the aggregation conditions, may switch the reaction between the available alternative pathways, and can thereby lead to the formation of structurally distinct prion aggregates.

Although the exact relationship of *in vitro* prion aggregation to prion-mediated cell toxicity awaits future studies, the principles of prion aggregation, emerging from the *in vitro* studies, appear to provide potentially the molecular basis of prion infection, replication, as well as the origin of prion strains. It is, however, important to note that similar principles underlie the amyloid fibril formation reactions of many other proteins. The parallel in-register structure, that potentially defines the molecular basis of the infectious nature of the prion protein, is the most common fold of amyloid fibrils, and amyloid fibrils of many other proteins possess this fold. It is increasingly becoming evident that structural heterogeneity as well as template-assisted conformational changes, are characteristics of protein aggregation by many other proteins[134,193–195], whose aggregates appear infectious in cell culture, as well as upon grafting and injection into animals[188,196–205]. It is not clear as to why infectiousness is restricted only to the prion protein in nature, and why other amyloidogenic proteins do not appear to be infectious. Future studies may clarify whether the infectious nature of the prion protein originates from the presence of its C-terminal GPI anchor[206], which is absent in other amyloid-forming proteins.

1. Chesebro, B. *et al.*, Identification of scrapie prion protein-specific mRNA in scrapie-infected and uninfected brain. *Nature*, 1985, **315**, 331–333.
2. Oesch, B. *et al.*, A cellular gene encodes scrapie PrP 27–30 protein. *Cell*, 1985, **40**, 735–746.
3. Kretzschmar, H. A., Prusiner, S. B., Stowring, L. E. and DeArmond, S. J., Scrapie prion proteins are synthesized in neurons. *Am. J. Pathol*., 1986, **122**, 1–5.
4. Stahl, N., Borchelt, D. R., Hsiao, K. and Prusiner, S. B., Scrapie prion protein contains a phosphatidylinositol glycolipid. *Cell*, 1987, **51**, 229–240.
5. Miura, T., Hori-i, A. and Takeuchi, H., Metal-dependent alpha-helix formation promoted by the glycine-rich octapeptide region of prion protein. *FEBS Lett*., 1996, **396**, 248–252.
6. Riek, R., Hornemann, S., Wider, G., Glockshuber, R. and Wuthrich, K., NMR characterization of the full-length recombinant murine prion protein, mPrP (23–231). *FEBS Lett*., 1997, **413**, 282–288.
7. Stockel, J., Safar, J., Wallace, A. C., Cohen, F. E. and Prusiner, S. B., Prion protein selectively binds copper(II) ions. *Biochemistry*, 1998, **37**, 7185–7193.
8. Chiesa, R. and Harris, D. A., Fishing for prion protein function. *PLoS Biol*., 2009, **7**, e75.

9. Bremer, J. *et al.*, Axonal prion protein is required for peripheral myelin maintenance. *Nature Neurosci*., 2010, **13**, 310–318.
10. Prusiner, S. B., Novel proteinaceous infectious particles cause scrapie. *Science*, 1982, **216**, 136–144.
11. Prusiner, S. B., Prions. *Proc. Natl. Acad. Sci. USA*, 1998, **95**, 13363–13383.
12. Creutzfeldt, H. G., Uber eine eigenartige herdformige Erkrankung des Zentralnervensystems. *Z. Gesamte Neurol. Psychiatr*., 1920, **57**, 1–18.
13. Jakob, A., Uber eigenartige Erkrankungen des Zentralnervensystems mit bemerkenswertem anatomischen Befunde (spatische Pseudoskelerose-Encephalomyelopathie mit disseminierten Degenerationsherden). *Z. Gesamte Neurol. Psychiatr*., 1921, **64**, 147–228.
14. Kirschbaum, W. R., *Jakob–Creutzfeldt Disease*, Elsevier, Amsterdam, 1968.
15. Klatzo, I., Gajdusek, D. C. and Zigas, V., Pathology of Kuru. *Lab. Invest*., 1959, **8**, 799–847.
16. Hadlow, W. J., Myopathies of livestock. *Lab. Invest*., 1959, **8**, 1478–1498.
17. Gordon, W. S., Advances in veterinary research. *Vet. Rec*., 1946, **58**, 516–525.
18. Sigurdsson, B., Rida, a chronic encephalitis of sheep with general remarks on infections which develop slowly and some of their special characteristics. *Br. Vet. J*., 1954, **110**, 341–354.
19. Hadlow, W. J., Neuropathology and the scrapie–kuru connection. *Brain Pathol*., 1995, **5**, 27–31.
20. Alper, T., Haig, D. A. and Clarke, M. C., The exceptionally small size of the scrapie agent. *Biochem. Biophys. Res. Commun*., 1966, **22**, 278–284.
21. Alper, T., Cramp, W. A., Haig, D. A. and Clarke, M. C., Does the agent of scrapie replicate without nucleic acid? *Nature*, 1967, **214**, 764–766.
22. Latarjet, R., Muel, B., Haig, D. A., Clarke, M. C. and Alper, T., Inactivation of the scrapie agent by near monochromatic ultraviolet light. *Nature*, 1970, **227**, 1341–1343.
23. Gibbs Jr, C. J., Gajdusek, D. C. and Latarjet, R., Unusual resistance to ionizing radiation of the viruses of Kuru, Creutzfeldt–Jakob disease and scrapie. *Proc. Natl. Acad. Sci. USA*, 1978, **75**, 6268–6270.
24. Pattison, I. H., In *Slow, Latent and Temperate Virus Infections*, NINDB Monograph 2 (eds Gajdusek, D. C., Gibbs Jr, C. J. and Alpers, M. P.), US Government Printing Office, Washington, DC, 1965, pp. 249–257.
25. Gibbons, R. A. and Hunter, G. D., Nature of the scrapie agent. *Nature*, 1967, **215**, 1041–1043.
26. Griffith, J. S., Self-replication and scrapie. *Nature*, 1967, **215**, 1043–1044.
27. Pattison, I. H. and Jones, K. M., The possible nature of the transmissible agent of scrapie. *Vet. Rec*., 1967, **80**, 2–9.
28. Hunter, G. D., Kimberlin, R. H. and Gibbons, R. A., Scrapie: a modified membrane hypothesis. *J. Theor. Biol*., 1968, **20**, 355–357.
29. Field, E. J., Farmer, F., Caspary, E. A. and Joyce, G., Susceptibility of scrapie agent to ionizing radiation. *Nature*, 1969, **222**, 90–91.
30. Hunter, G. D., Scrapie: a prototype slow infection. *J. Infect. Dis*., 1972, **125**, 427–440.
31. Hunter, G. D. and Millson, G. C., Attempts to release the scrapie agent from tissue debris. *J. Comp. Pathol*., 1967, **77**, 301–307.
32. Prusiner, S. B., Groth, D. F., Cochran, S. P., Masiarz, F. R., McKinley, M. P. and Martinez, H. M., Molecular properties, partial purification, and assay by incubation period measurements of the hamster scrapie agent. *Biochemistry*, 1980, **19**, 4883–4891.
33. Prusiner, S. B., Groth, D. F., McKinley, M. P., Cochran, S. P., Bowman, K. A. and Kasper, K. C., Thiocyanate and hydroxyl ions inactivate the scrapie agent. *Proc. Natl. Acad. Sci. USA*, 1981, **78**, 4606–4610.
34. Bolton, D. C., McKinley, M. P. and Prusiner, S. B., Identification of a protein that purifies with the scrapie prion. *Science*, 1982, **218**, 1309–1311.
35. Prusiner, S. B., Groth, D. F., Bolton, D. C., Kent, S. B. and Hood, L. E., Purification and structural studies of a major scrapie prion protein. *Cell*, 1984, **38**, 127–134.
36. Basler, K. *et al.*, Scrapie and cellular PrP isoforms are encoded by the same chromosomal gene. *Cell*, 1986, **46**, 417–428.
37. Locht, C., Chesebro, B., Race, R. and Keith, J. M., Molecular cloning and complete sequence of prion protein cDNA from mouse brain infected with the scrapie agent. *Proc. Natl. Acad. Sci. USA*, 1986, **83**, 6372–6376.
38. Meyer, R. K., McKinley, M. P., Bowman, K. A., Braunfeld, M. B., Barry, R. A. and Prusiner, S. B., Separation and properties of cellular and scrapie prion proteins. *Proc. Natl. Acad. Sci. USA*, 1986, **83**, 2310–2314.
39. Bueler, H. *et al.*, Normal development and behaviour of mice lacking the neuronal cell-surface PrP protein. *Nature*, 1992, **356**, 577–582.
40. Bueler, H., Aguzzi, A., Sailer, A., Greiner, R. A., Autenried, P., Aguet, M. and Weissmann, C., Mice devoid of PrP are resistant to scrapie. *Cell*, 1993, **73**, 1339–1347.
41. Westaway, D. *et al.*, Degeneration of skeletal muscle, peripheral nerves, and the central nervous system in transgenic mice overexpressing wild-type prion proteins. *Cell*, 1994, **76**, 117–129.
42. Wang, F., Wang, X., Yuan, C. G. and Ma, J., Generating a prion with bacterially expressed recombinant prion protein. *Science*, 2010, **327**, 1132–1135.
43. Kim, J. I. *et al.*, Mammalian prions generated from bacterially expressed prion protein in the absence of any mammalian cofactors. *J. Biol. Chem*., 2010, **285**, 14083–14087.
44. Eanes, E. D. and Glenner, G. G., X-ray diffraction studies on amyloid filaments. *J. Histochem. Cytochem*., 1968, **16**, 673–677.
45. Sunde, M., Serpell, L. C., Bartlam, M., Fraser, P. E., Pepys, M. B. and Blake, C. C., Common core structure of amyloid fibrils by synchrotron X-ray diffraction. *J. Mol. Biol*., 1997, **273**, 729–739.
46. Selkoe, D. J., Folding proteins in fatal ways. *Nature*, 2003, **426**, 900–904.
47. Chiti, F. and Dobson, C. M., Protein misfolding, functional amyloid, and human disease. *Annu. Rev. Biochem*., 2006, **75**, 333–366.
48. Pan, K. M. *et al.*, Conversion of alpha-helices into beta-sheets features in the formation of the scrapie prion proteins. *Proc. Natl. Acad. Sci. USA*, 1993, **90**, 10962–10966.
49. Peretz, D., Scott, M. R., Groth, D., Williamson, R. A., Burton, D. R., Cohen, F. E. and Prusiner, S. B., Strain-specified relative conformational stability of the scrapie prion protein. *Protein Sci*., 2001, **10**, 854–863.
50. Prusiner, S. B., Bolton, D. C., Groth, D. F., Bowman, K. A., Cochran, S. P. and McKinley, M. P., Further purification and characterization of scrapie prions. *Biochemistry*, 1982, **21**, 6942–6950.
51. Prusiner, S. B., McKinley, M. P., Bowman, K. A., Bolton, D. C., Bendheim, P. E., Groth, D. F. and Glenner, G. G., Scrapie prions aggregate to form amyloid-like birefringent rods. *Cell*, 1983, **35**, 349–358.
52. DeArmond, S. J., McKinley, M. P., Barry, R. A., Braunfeld, M. B., McColloch, J. R. and Prusiner, S. B., Identification of prion amyloid filaments in scrapie-infected brain. *Cell*, 1985, **41**, 221–235.
53. Kitamoto, T., Tateishi, J., Tashima, T., Takeshita, I., Barry, R. A., DeArmond, S. J. and Prusiner, S. B., Amyloid plaques in Creutzfeldt-Jakob disease stain with prion protein antibodies. *Ann. Neurol*., 1986, **20**, 204–208.

54. Roberts, G. W., Lofthouse, R., Brown, R., Crow, T. J., Barry, R. A. and Prusiner, S. B., Prion-protein immunoreactivity in human transmissible dementias. *N. Engl. J. Med*., 1986, **315**, 1231–1233.
55. Brandner, S., Raeber, A., Sailer, A., Blattler, T., Fischer, M., Weissmann, C. and Aguzzi, A., Normal host prion protein (PrPC) is required for scrapie spread within the central nervous system. *Proc. Natl. Acad. Sci. USA*, 1996, **93**, 13148–13151.
56. Mallucci, G., Dickinson, A., Linehan, J., Klohn, P. C., Brandner, S. and Collinge, J., Depleting neuronal PrP in prion infection prevents disease and reverses spongiosis. *Science*, 2003, **302**, 871–874.
57. Mallucci, G. R. *et al.*, Targeting cellular prion protein reverses early cognitive deficits and neurophysiological dysfunction in prion-infected mice. *Neuron*, 2007, **53**, 325–335.
58. Tateishi, J. and Kitamoto, T., Inherited prion diseases and transmission to rodents. *Brain Pathol*., 1995, **5**, 53–59.
59. Tateishi, J., Kitamoto, T., Hoque, M. Z. and Furukawa, H., Experimental transmission of Creutzfeldt–Jakob disease and related diseases to rodents. *Neurology*, 1996, **46**, 532–537.
60. Lasmezas, C. I. *et al.*, Transmission of the BSE agent to mice in the absence of detectable abnormal prion protein. *Science*, 1997, **275**, 402–405.
61. Chiesa, R. *et al.*, Molecular distinction between pathogenic and infectious properties of the prion protein. *J. Virol*., 2003, **77**, 7611–7622.
62. Gambetti, P. *et al.*, A novel human disease with abnormal prion protein sensitive to protease. *Ann. Neurol*., 2008, **63**, 697–708.
63. Head, M. W., Knight, R., Zeidler, M., Yull, H., Barlow, A. and Ironside, J. W., A case of protease sensitive prionopathy in a patient in the UK. *Neuropathol. Appl. Neurobiol*., 2009, **35**, 628–632.
64. Caughey, B. and Lansbury, P. T., Protofibrils, pores, fibrils, and neurodegeneration: separating the responsible protein aggregates from the innocent bystanders. *Annu. Rev. Neurosci*., 2003, **26**, 267–298.
65. Kayed, R., Head, E., Thompson, J. L., McIntire, T. M., Milton, S. C., Cotman, C. W. and Glabe, C. G., Common structure of soluble amyloid oligomers implies common mechanism of pathogenesis. *Science*, 2003, **300**, 486–489.
66. Kayed, R., Sokolov, Y., Edmonds, B., McIntire, T. M., Milton, S. C., Hall, J. E. and Glabe, C. G., Permeabilization of lipid bilayers is a common conformation-dependent activity of soluble amyloid oligomers in protein misfolding diseases. *J. Biol. Chem*., 2004, **279**, 46363–46366.
67. Silveira, J. R., Raymond, G. J., Hughson, A. G., Race, R. E., Sim, V. L., Hayes, S. F. and Caughey, B., The most infectious prion protein particles. *Nature*, 2005, **437**, 257–261.
68. Novitskaya, V., Bocharova, O. V., Bronstein, I. and Baskakov, I. V., Amyloid fibrils of mammalian prion protein are highly toxic to cultured cells and primary neurons. *J. Biol. Chem*., 2006, **281**, 13828–13836.
69. Xue, W. F., Hellewell, A. L., Gosal, W. S., Homans, S. W., Hewitt, E. W. and Radford, S. E., Fibril fragmentation enhances amyloid cytotoxicity. *J. Biol. Chem*., 2009, **284**, 34272–34282.
70. Riek, R., Hornemann, S., Wider, G., Billeter, M., Glockshuber, R. and Wuthrich, K., NMR structure of the mouse prion protein domain PrP(121–321). *Nature*, 1996, **382**, 180–182.
71. Stahl, N., Baldwin, M. A., Teplow, D. B., Hood, L., Gibson, B. W., Burlingame, A. L. and Prusiner, S. B., Structural studies of the scrapie prion protein using mass spectrometry and amino acid sequencing. *Biochemistry*, 1993, **32**, 1991–2002.
72. Baldwin, M. A., Mass spectrometric analysis of prion proteins. *Adv. Protein Chem.*, 2001, **57**, 29–54.
73. Peretz, D. *et al.*, A conformational transition at the N terminus of the prion protein features in formation of the scrapie isoform. *J. Mol. Biol*., 1997, **273**, 614–622.
74. Wille, H. *et al.*, Structural studies of the scrapie prion protein by electron crystallography. *Proc. Natl. Acad. Sci. USA*, 2002, **99**, 3563–3568.
75. Govaerts, C., Wille, H., Prusiner, S. B. and Cohen, F. E., Evidence for assembly of prions with left-handed beta-helices into trimers. *Proc. Natl. Acad. Sci. USA*, 2004, **101**, 8342–8347.
76. DeMarco, M. L. and Daggett, V., From conversion to aggregation: protofibril formation of the prion protein. *Proc. Natl. Acad. Sci. USA*, 2004, **101**, 2293–2298.
77. DeMarco, M. L., Silveira, J., Caughey, B. and Daggett, V., Structural properties of prion protein protofibrils and fibrils: an experimental assessment of atomic models. *Biochemistry*, 2006, **45**, 15573–15582.
78. Dima, R. I. and Thirumalai, D., Exploring the propensities of helices in PrP(C) to form beta sheet using NMR structures and sequence alignments. *Biophys. J*., 2002, **83**, 1268–1280.
79. Dima, R. I. and Thirumalai, D., Probing the instabilities in the dynamics of helical fragments from mouse PrPC. *Proc. Natl. Acad. Sci. USA*, 2004, **101**, 15335–15340.
80. Legname, G., Baskakov, I. V., Nguyen, H. O., Riesner, D., Cohen, F. E., DeArmond, S. J. and Prusiner, S. B., Synthetic mammalian prions. *Science*, 2004, **305**, 673–676.
81. Lu, X., Wintrode, P. L. and Surewicz, W. K., Beta-sheet core of human prion protein amyloid fibrils as determined by hydrogen/deuterium exchange. *Proc. Natl. Acad. Sci. USA*, 2007, **104**, 1510–1515.
82. Cobb, N. J., Sonnichsen, F. D., McHaourab, H. and Surewicz, W. K., Molecular architecture of human prion protein amyloid: a parallel, in-register beta-structure. *Proc. Natl. Acad. Sci. USA*, 2007, **104**, 18946–18951.
83. Tycko, R., Savtchenko, R., Ostapchenko, V. G., Makarava, N. and Baskakov, I. V., The alpha-helical C-terminal domain of full-length recombinant PrP converts to an in-register parallel beta-sheet structure in PrP fibrils: evidence from solid state nuclear magnetic resonance. *Biochemistry*, 2010, **49**, 9488–9497.
84. Antzutkin, O. N., Balbach, J. J., Leapman, R. D., Rizzo, N. W., Reed, J. and Tycko, R., Multiple quantum solid-state NMR indicates a parallel, not antiparallel, organization of beta-sheets in Alzheimer's beta-amyloid fibrils. *Proc. Natl. Acad. Sci. USA*, 2000, **97**, 13045–13050.
85. Petkova, A. T., Ishii, Y., Balbach, J. J., Antzutkin, O. N., Leapman, R. D., Delaglio, F. and Tycko, R., A structural model for Alzheimer's beta-amyloid fibrils based on experimental constraints from solid state NMR. *Proc. Natl. Acad. Sci. USA*, 2002, **99**, 16742–16747.
86. Der-Sarkissian, A., Jao, C. C., Chen, J. and Langen, R., Structural organization of alpha-synuclein fibrils studied by site-directed spin labelling. *J. Biol. Chem*., 2003, **278**, 37530–37535.
87. Margittai, M. and Langen, R., Template-assisted filament growth by parallel stacking of tau. *Proc. Natl. Acad. Sci. USA*, 2004, **101**, 10278–10283.
88. Jha, A., Udgaonkar, J. B. and Krishnamoorthy, G., Characterization of the heterogeneity and specificity of interpolypeptide interactions in amyloid protofibrils by measurement of site-specific fluorescence anisotropy decay kinetics. *J. Mol. Biol*., 2009, **393**, 735–752.
89. Shewmaker, F., Wickner, R. B. and Tycko, R., Amyloid of the prion domain of Sup35p has an in-register parallel beta-sheet structure. *Proc. Natl. Acad. Sci. USA*, 2006, **103**, 19754–19759.
90. Baxa, U., Wickner, R. B., Steven, A. C., Anderson, D. E., Marekov, L. N., Yau, W. M. and Tycko, R., Characterization of beta-sheet structure in Ure2p1-89 yeast prion fibrils by solid-state nuclear magnetic resonance. *Biochemistry*, 2007, **46**, 13149–13162.
91. Wickner, R. B., Dyda, F. and Tycko, R., Amyloid of Rnq1p, the basis of the [PIN$^+$] prion, has a parallel in-register beta-sheet structure. *Proc. Natl. Acad. Sci. USA*, 2008, **105**, 2403–2408.

92. Helmus, J. J., Surewicz, K., Nadaud, P. S., Surewicz, W. K. and Jaroniec, C. P., Molecular conformation and dynamics of the Y145Stop variant of human prion protein in amyloid fibrils. *Proc. Natl. Acad. Sci. USA*, 2008, **105**, 6284–6289.
93. Lim, K. H. *et al.*, Solid-state NMR structural studies of the fibril form of a mutant mouse prion peptide PrP89-143(P101L). *Solid State Nucl. Magn. Reson*., 2006, **29**, 183–190.
94. Damo, S. M., Phillips, A. H., Young, A. L., Li, S., Woods Jr, V. L. and Wemmer, D. E., Probing the conformation of a prion protein fibril with hydrogen exchange. *J. Biol. Chem*., 2010, **285**, 32303–32311.
95. Shewmaker, F., Kryndushkin, D., Chen, B., Tycko, R. and Wickner, R. B., Two prion variants of Sup35p have in-register parallel beta-sheet structures, independent of hydration. *Biochemistry*, 2009, **48**, 5074–5082.
96. Legname, G., Nguyen, H. O., Baskakov, I. V., Cohen, F. E., Dearmond, S. J. and Prusiner, S. B., Strain-specified characteristics of mouse synthetic prions. *Proc. Natl. Acad. Sci. USA*, 2005, **102**, 2168–2173.
97. Smirnovas, V., Baron, G. S., Offerdahl, D. K., Raymond, G. J., Caughey, B. and Surewicz, W. K., Structural organization of brain-derived mammalian prions examined by hydrogen–deuterium exchange. *Nature Struct. Mol. Biol*., 2011, **18**, 504–506.
98. Booth, D. R. *et al.*, Instability, unfolding and aggregation of human lysozyme variants underlying amyloid fibrillogenesis. *Nature*, 1997, **385**, 787–793.
99. Kelly, J. W., The alternative conformations of amyloidogenic proteins and their multi-step assembly pathways. *Curr. Opin. Struct. Biol*., 1998, **8**, 101–106.
100. Uversky, V. N. and Fink, A. L., Conformational constraints for amyloid fibrillation: the importance of being unfolded. *Biochim. Biophys. Acta*, 2004, **1698**, 131–153.
101. Liu, K., Cho, H. S., Lashuel, H. A., Kelly, J. W. and Wemmer, D. E., A glimpse of a possible amyloidogenic intermediate of transthyretin. *Nature Struct. Biol*., 2000, **7**, 754–757.
102. McParland, V. J., Kalverda, A. P., Homans, S. W. and Radford, S. E., Structural properties of an amyloid precursor of beta(2)-microglobulin. *Nature Struct. Biol*., 2002, **9**, 326–331.
103. Gianni, S., Ivarsson, Y., De Simone, A., Travaglini-Allocatelli, C., Brunori, M. and Vendruscolo, M., Structural characterization of a misfolded intermediate populated during the folding process of a PDZ domain. *Nature Struct. Mol. Biol*., 2010, **17**, 1431–1437.
104. Chiti, F. and Dobson, C. M., Amyloid formation by globular proteins under native conditions. *Nature Chem. Biol*., 2009, **5**, 15–22.
105. Bishop, M. F. and Ferrone, F. A., Kinetics of nucleation-controlled polymerization. A perturbation treatment for use with a secondary pathway. *Biophys. J*., 1984, **46**, 631–644.
106. Oosawa, F. and Kasai, M., A theory of linear and helical aggregations of macromolecules. *J. Mol. Biol*., 1962, **4**, 10–21.
107. Harper, J. D. and Lansbury Jr, P. T., Models of amyloid seeding in Alzheimer's disease and scrapie: mechanistic truths and physiological consequences of the time-dependent solubility of amyloid proteins. *Annu. Rev. Biochem*., 1997, **66**, 385–407.
108. Ferrone, F., Analysis of protein aggregation kinetics. *Methods Enzymol*., 1999, **309**, 256–274.
109. Kumar, S. and Udgaonkar, J. B., Mechanisms of amyloid fibril formation by proteins. *Curr. Sci*., 2010, **98**, 639–656.
110. Romberg, L., Simon, M. and Erickson, H. P., Polymerization of Ftsz, a bacterial homolog of tubulin, assembly cooperative? *J. Biol. Chem*., 2001, **276**, 11743–11753.
111. Frieden, C., Protein aggregation processes: in search of the mechanism. *Protein Sci*., 2007, **16**, 2334–2344.
112. Serio, T. R. *et al.*, Nucleated conformational conversion and the replication of conformational information by a prion determinant. *Science*, 2000, **289**, 1317–1321.
113. Collins, S. R., Douglass, A., Vale, R. D. and Weissman, J. S., Mechanism of prion propagation: amyloid growth occurs by monomer addition. *PLoS Biol*., 2004, **2**, e321.
114. Baskakov, I. V. and Bocharova, O. V., *In vitro* conversion of mammalian prion protein into amyloid fibrils displays unusual features. *Biochemistry*, 2005, **44**, 2339–2348.
115. Bhattacharyya, A. M., Thakur, A. K. and Wetzel, R., Polyglutamine aggregation nucleation: thermodynamics of a highly unfavourable protein folding reaction. *Proc. Natl. Acad. Sci. USA*, 2005, **102**, 15400–15405.
116. Xue, W. F., Homans, S. W. and Radford, S. E., Systematic analysis of nucleation-dependent polymerization reveals new insights into the mechanism of amyloid self-assembly. *Proc. Natl. Acad. Sci. USA*, 2008, **105**, 8926–8931.
117. Chen, S., Ferrone, F. A. and Wetzel, R., Huntington's disease age-of-onset linked to polyglutamine aggregation nucleation. *Proc. Natl. Acad. Sci. USA*, 2002, **99**, 11884–11889.
118. Ferrone, F. A., Hofrichter, J., Sunshine, H. R. and Eaton, W. A., Kinetic studies on photolysis-induced gelation of sickle cell hemoglobin suggest a new mechanism. *Biophys. J*., 1980, **32**, 361–380.
119. Wegner, A., Spontaneous fragmentation of actin filaments in physiological conditions. *Nature*, 1982, **296**, 266–267.
120. Wegner, A. and Savko, P., Fragmentation of actin filaments. *Biochemistry*, 1982, **21**, 1909–1913.
121. Modler, A. J., Gast, K., Lutsch, G. and Damaschun, G., Assembly of amyloid protofibrils via critical oligomers – a novel pathway of amyloid formation. *J. Mol. Biol*., 2003, **325**, 135–148.
122. Kumar, S. and Udgaonkar, J. B., Structurally distinct amyloid protofibrils form on separate pathways of aggregation of a small protein. *Biochemistry*, 2009, **48**, 6441–6449.
123. Kumar, S. and Udgaonkar, J. B., Conformational conversion may precede or follow aggregate elongation on alternative pathways of amyloid protofibril formation. *J. Mol. Biol*., 2009, **385**, 1266–1276.
124. Walsh, D. M., Lomakin, A., Benedek, G. B., Condron, M. M. and Teplow, D. B., Amyloid beta-protein fibrillogenesis. Detection of a protofibrillar intermediate. *J. Biol. Chem*., 1997, **272**, 22364–22372.
125. Walsh, D. M. *et al.*, Amyloid beta-protein fibrillogenesis. Structure and biological activity of protofibrillar intermediates. *J. Biol. Chem*., 1999, **274**, 25945–25952.
126. Kheterpal, I., Chen, M., Cook, K. D. and Wetzel, R., Structural differences in Aβ amyloid protofibrils and fibrils mapped by hydrogen exchange-mass spectrometry with on-line proteolytic fragmentation. *J. Mol. Biol*., 2006, **361**, 785–795.
127. Chimon, S., Shaibat, M. A., Jones, C. R., Calero, D. C., Aizezi, B. and Ishii, Y., Evidence of fibril-like beta-sheet structures in a neurotoxic amyloid intermediate of Alzheimer's beta-amyloid. *Nature Struct. Mol. Biol*., 2007, **14**, 1157–1164.
128. Jain, S. and Udgaonkar, J. B., Evidence for stepwise formation of amyloid fibrils by the mouse prion protein. *J. Mol. Biol*., 2008, **382**, 1228–1241.
129. Jain, S. and Udgaonkar, J. B., Defining the pathway of worm-like amyloid fibril formation by the mouse prion protein by delineation of the productive and unproductive oligomerization reactions. *Biochemistry*, 2011, **50**, 1153–1161.
130. Esler, W. P. *et al.*, Alzheimer's disease amyloid propagation by a template-dependent dock-lock mechanism. *Biochemistry*, 2000, **39**, 6288–6295.
131. Scheibel, T., Bloom, J. and Lindquist, S. L., The elongation of yeast prion fibers involves separable steps of association and conversion. *Proc. Natl. Acad. Sci. USA*, 2004, **101**, 2287–2292.

132. Kumar, S., Mohanty, S. K. and Udgaonkar, J. B., Mechanism of formation of amyloid protofibrils of barstar from soluble oligomers: evidence for multiple steps and lateral association coupled to conformational conversion. *J. Mol. Biol*., 2007, **367**, 1186–1204.
133. Jain, S. and Udgaonkar, J. B., Salt-induced modulation of the pathway of amyloid fibril formation by the mouse prion protein. *Biochemistry*, 2010, **49**, 7615–7624.
134. Toyama, B. H. and Weissman, J. S., Amyloid structure: conformational diversity and consequences. *Annu. Rev. Biochem*., 2011, **80**, 557–585.
135. Prusiner, S. B., Molecular biology of prion diseases. *Science*, 1991, **252**, 1515–1522.
136. Jarrett, J. T. and Lansbury Jr, P. T., Seeding 'one-dimensional crystallization' of amyloid: a pathogenic mechanism in Alzheimer's disease and scrapie? *Cell*, 1993, **73**, 1055–1058.
137. Weissmann, C., The state of the prion. *Nature Rev. Microbiol*., 2004, **2**, 861–871.
138. Pattison, I. H. and Millson, G. C., Scrapie produced experimentally in goats with special reference to the clinical syndrome. *J. Comp. Pathol*., 1961, **71**, 101–108.
139. Fraser, H. and Dickinson, A. G., The sequential development of the brain lesion of scrapie in three strains of mice. *J. Comp. Pathol*., 1968, **78**, 301–311.
140. Fraser, H. and Dickinson, A. G., Scrapie in mice. Agent-strain differences in the distribution and intensity of grey matter vacuolation. *J. Comp. Pathol*., 1973, **83**, 29–40.
141. Hecker, R. *et al.*, Replication of distinct scrapie prion isolates is region specific in brains of transgenic mice and hamsters. *Genes Dev*., 1992, **6**, 1213–1228.
142. DeArmond, S. J., Yang, S. L., Lee, A., Bowler, R., Taraboulos, A., Groth, D. and Prusiner, S. B., Three scrapie prion isolates exhibit different accumulation patterns of the prion protein scrapie isoform. *Proc. Natl. Acad. Sci. USA*, 1993, **90**, 6449–6453.
143. Collinge, J., Prion diseases of humans and animals: their causes and molecular basis. *Annu. Rev. Neurosci*., 2001, **24**, 519–550.
144. Bessen, R. A. and Marsh, R. F., Distinct PrP properties suggest the molecular basis of strain variation in transmissible mink encephalopathy. *J. Virol.*, 1994, **68**, 7859–7868.
145. Caughey, B., Raymond, G. J. and Bessen, R. A., Strain-dependent differences in beta-sheet conformations of abnormal prion protein. *J. Biol. Chem*., 1998, **273**, 32230–32235.
146. Safar, J. *et al.*, Eight prion strains have PrP(Sc) molecules with different conformations. *Nature Med.*, 1998, **4**, 1157–1165.
147. Somerville, R. A., TSE agent strains and PrP: reconciling structure and function. *Trends Biochem. Sci*., 2002, **27**, 606–612.
148. Bruce, M. E. and Fraser, H., Scrapie strain variation and its implications. *Curr. Top. Microbiol. Immunol*., 1991, **172**, 125–138.
149. Priola, S. A. and Lawson, V. A., Glycosylation influences cross-species formation of protease-resistant prion protein. *EMBO J*., 2001, **20**, 6692–6699.
150. Vorberg, I. and Priola, S. A., Molecular basis of scrapie strain glycoform variation. *J. Biol. Chem*., 2002, **277**, 36775–36781.
151. Chien, P., Weissman, J. S. and DePace, A. H., Emerging principles of conformation-based prion inheritance. *Annu. Rev. Biochem*., 2004, **73**, 617–656.
152. Hornemann, S., Schorn, C. and Wuthrich, K., NMR structure of the bovine prion protein isolated from healthy calf brains. *EMBO Rep*., 2004, **5**, 1159–1164.
153. Wildegger, G., Liemann, S. and Glockshuber, R., Extremely rapid folding of the C-terminal domain of the prion protein without kinetic intermediates. *Nature Struct. Biol*., 1999, **6**, 550–553.
154. Apetri, A. C. and Surewicz, W. K., Kinetic intermediate in the folding of human prion protein. *J. Biol. Chem*., 2002, **277**, 44589–44592.
155. Apetri, A. C., Maki, K., Roder, H. and Surewicz, W. K., Early intermediate in human prion protein folding as evidenced by ultrarapid mixing experiments. *J. Am. Chem. Soc*., 2006, **128**, 11673–11678.
156. Nicholson, E. M., Mo, H., Prusiner, S. B., Cohen, F. E. and Marqusee, S., Differences between the prion protein and its homolog Doppel: a partially structured state with implications for scrapie formation. *J. Mol. Biol*., 2002, **316**, 807–815.
157. Kuwata, K., Li, H., Yamada, H., Legname, G., Prusiner, S. B., Akasaka, K. and James, T. L., Locally disordered conformer of the hamster prion protein: a crucial intermediate to PrPSc? *Biochemistry*, 2002, **41**, 12277–12283.
158. Kocisko, D. A., Come, J. H., Priola, S. A., Chesebro, B., Raymond, G. J., Lansbury, P. T. and Caughey, B., Cell-free formation of protease-resistant prion protein. *Nature*, 1994, **370**, 471–474.
159. Cohen, F. E., Pan, K. M., Huang, Z., Baldwin, M., Fletterick, R. J. and Prusiner, S. B., Structural clues to prion replication. *Science*, 1994, **264**, 530–531.
160. Swietnicki, W., Petersen, R. B., Gambetti, P. and Surewicz, W. K., Familial mutations and the thermodynamic stability of the recombinant human prion protein. *J. Biol. Chem*., 1998, **273**, 31048–31052.
161. Apetri, A. C., Surewicz, K. and Surewicz, W. K., The effect of disease-associated mutations on the folding pathway of human prion protein. *J. Biol. Chem*., 2004, **279**, 18008–18014.
162. Morillas, M., Vanik, D. L. and Surewicz, W. K., On the mechanism of alpha-helix to beta-sheet transition in the recombinant prion protein. *Biochemistry*, 2001, **40**, 6982–6987.
163. Caughey, B., Raymond, G. J., Ernst, D. and Race, R. E., N-terminal truncation of the scrapie-associated form of PrP by lysosomal protease(s): implications regarding the site of conversion of PrP to the protease-resistant state. *J. Virol*., 1991, **65**, 6597–6603.
164. Borchelt, D. R., Taraboulos, A. and Prusiner, S. B., Evidence for synthesis of scrapie prion proteins in the endocytic pathway. *J. Biol. Chem*., 1992, **267**, 16188–16199.
165. Swietnicki, W., Petersen, R., Gambetti, P. and Surewicz, W. K., pH-dependent stability and conformation of the recombinant human prion protein PrP (90–231). *J. Biol. Chem*., 1997, **272**, 27517–27520.
166. Swietnicki, W., Morillas, M., Chen, S. G., Gambetti, P. and Surewicz, W. K., Aggregation and fibrillization of the recombinant human prion protein huPrP90–231. *Biochemistry*, 2000, **39**, 424–431.
167. Baskakov, I. V., Legname, G., Prusiner, S. B. and Cohen, F. E., Folding of prion protein to its native alpha-helical conformation is under kinetic control. *J. Biol. Chem*., 2001, **276**, 19687–19690.
168. Baskakov, I. V., Legname, G., Baldwin, M. A., Prusiner, S. B. and Cohen, F. E., Pathway complexity of prion protein assembly into amyloid. *J. Biol. Chem*., 2002, **277**, 21140–21148.
169. Baskakov, I. V., Autocatalytic conversion of recombinant prion proteins displays a species barrier. *J. Biol. Chem*., 2004, **279**, 7671–7677.
170. Bocharova, O. V., Breydo, L., Parfenov, A. S., Salnikov, V. V. and Baskakov, I. V., *In vitro* conversion of full-length mammalian prion protein produces amyloid form with physical properties of PrP(Sc). *J. Mol. Biol*., 2005, **346**, 645–659.
171. Jackson, G. S. *et al.*, Reversible conversion of monomeric human prion protein between native and fibrilogenic conformations. *Science*, 1999, **283**, 1935–1937.
172. Maiti, N. R. and Surewicz, W. K., The role of disulfide bridge in the folding and stability of the recombinant human prion protein. *J. Biol. Chem*., 2001, **276**, 2427–2431.
173. Rezaei, H., Eghiaian, F., Perez, J., Doublet, B., Choiset, Y., Haertle, T. and Grosclaude, J., Sequential generation of two

structurally distinct ovine prion protein soluble oligomers displaying different biochemical reactivities. *J. Mol. Biol*., 2005, **347**, 665–679.
174. Vendrely, C. *et al.*, Assembly of the full-length recombinant mouse prion protein I. Formation of soluble oligomers. *Biochim. Biophys. Acta*, 2005, **1724**, 355–366.
175. Eghiaian, F. *et al*., Diversity in prion protein oligomerization pathways results from domain expansion as revealed by hydrogen/deuterium exchange and disulfide linkage. *Proc. Natl. Acad. Sci. USA*, 2007, **104**, 7414–7419.
176. Anderson, M., Bocharova, O. V., Makarava, N., Breydo, L., Salnikov, V. V. and Baskakov, I. V., Polymorphism and ultrastructural organization of prion protein amyloid fibrils: an insight from high resolution atomic force microscopy. *J. Mol. Biol*., 2006, **358**, 580–596.
177. Colby, D. W., Giles, K., Legname, G., Wille, H., Baskakov, I. V., DeArmond, S. J. and Prusiner, S. B., Design and construction of diverse mammalian prion strains. *Proc. Natl. Acad. Sci. USA*, 2009, **106**, 20417–20422.
178. Makarava, N. and Baskakov, I. V., The same primary structure of the prion protein yields two distinct self-propagating states. *J. Biol. Chem*., 2008, **283**, 15988–15996.
179. Ostapchenko, V. G., Makarava, N., Savtchenko, R. and Baskakov, I. V., The polybasic N-terminal region of the prion protein controls the physical properties of both the cellular and fibrillar forms of PrP. *J. Mol. Biol*., 2008, **383**, 1210–1224.
180. Ostapchenko, V. G., Sawaya, M. R., Makarava, N., Savtchenko, R., Nilsson, K. P., Eisenberg, D. and Baskakov, I. V., Two amyloid states of the prion protein display significantly different folding patterns. *J. Mol. Biol*., 2010, **400**, 908–921.
181. Gosal, W. S., Morten, I. J., Hewitt, E. W., Smith, D. A., Thomson, N. H. and Radford, S. E., Competing pathways determine fibril morphology in the self-assembly of beta2-microglobulin into amyloid. *J. Mol. Biol*., 2005, **351**, 850–864.
182. Apetri, A. C., Vanik, D. L. and Surewicz, W. K., Polymorphism at residue 129 modulates the conformational conversion of the D178N variant of human prion protein 90–231. *Biochemistry*, 2005, **44**, 15880–15888.
183. Cobb, N. J., Apetri, A. C. and Surewicz, W. K., Prion protein amyloid formation under native like conditions involves refolding of the C-terminal α-helical domain. *J. Biol. Chem*., 2008, **283**, 34704–34711.
184. Prusiner, S. B., *Prion Biology and Diseases*, Cold Spring Harbor, Monograph Series, 2004.
185. Wickner, R. B., Edskes, H. K., Shewmaker, F. and Nakayashiki, T., Prions of fungi: inherited structures and biological roles. *Nature Rev. Microbiol*., 2007, **5**, 611–618.
186. Wickner, R. B. *et al.*, Prion amyloid structure explains templating: how proteins can be genes. *FEMS Yeast Res.*, 2010, **10**, 980–991.
187. Wiltzius, J. J. W. *et al.*, Molecular mechanisms for protein-encoded inheritance. *Nature Struct. Mol. Biol*., 2009, **16**, 973–979.
188. Li, J., Browning, S., Mahal, S. P., Oelschlegel, A. M. and Weissmann, C., Darwinian evolution of prions in cell culture. *Science*, 2010, **327**, 869–872.
189. Vanik, D. L., Surewicz, K. A. and Surewicz, W. K., Molecular basis of barriers for interspecies transmissibility of mammalian prions. *Mol. Cell*, 2004, **14**, 139–145.
190. Jones, E. M. and Surewicz, W. K., Fibril conformation as the basis of species- and strain-dependent seeding specificity of mammalian prion amyloids. *Cell*, 2005, **121**, 63–72.
191. Kundu, B., Maiti, N. R., Jones, E. M., Surewicz, K. A., Vanik, D. L. and Surewicz, W. K., Nucleation-dependent conformational conversion of the Y145Stop variant of human prion protein: structural clues for prion propagation. *Proc. Natl. Acad. Sci. USA*, 2003, **100**, 12069–12074.
192. Apostol, M. I., Wiltzius, J. J. W., Sawaya, M. R., Cascio, D. and Eisenberg, D., Atomic structures suggest determinants of transmission barriers in mammalian prion disease. *Biochemistry*, 2011, **50**, 2456–2463.
193. Aoyagi, H., Hasegawa, M. and Tamaoka, A., Fibrillogenic nuclei composed of P301L mutant tau induce elongation of P301L tau but not wild-type tau. *J. Biol. Chem*., 2007, **282**, 20309–20318.
194. Frost, B., Ollesch, J., Wille, H. and Diamond, M. I., Conformational diversity of wild-type Tau fibrils specified by templated conformation change. *J. Biol. Chem*., 2009, **284**, 3546–3551.
195. Frost, B. and Diamond, M. I., The expanding realm of prion phenomena in neurodegenerative disease. *Prion*, 2009, **3**, 74–77.
196. Kane, M. D. *et al*., Evidence for seeding of beta-amyloid by intracerebral infusion of Alzheimer brain extracts in beta-amyloid precursor protein-transgenic mice. *J. Neurosci*., 2000, **20**, 3606–3611.
197. Goedert, M., Spillantini, M. G., Serpell, L. C., Berriman, J., Smith, M. J., Jakes, R. and Crowther, R. A., From genetics to pathology: tau and alpha-synuclein assemblies in neurodegenerative diseases. *Philos. Trans. R. Soc. London B Biol. Sci*., 2001, **356**, 213–227.
198. Walker, L. C., Callahan, M. J., Bian, F., Durham, R. A., Roher, A. E. and Lipinski, W. J., Exogenous induction of cerebral beta-amyloidosis in betaAPP-transgenic mice. *Peptides*, 2002, **23**, 1241–1247.
199. Yang, W., Dunlap, J. R., Andrews, R. B. and Wetzel, R., Aggregated polyglutamine peptides delivered to nuclei are toxic to mammalian cells. *Hum. Mol. Genet*., 2002, **11**, 2905–2917.
200. Braak, H., Del Tredici, K., Rub, U., de Vos, R. A., Jansen Steur, E. N. and Braak, E., Staging of brain pathology related to sporadic Parkinson's disease. *Neurobiol. Aging*, 2003, **24**, 197–211.
201. Brouwers, N., Sleegers, K. and Van Broeckhoven, C., Molecular genetics of Alzheimer's disease: an update. *Annu. Med*., 2008, **40**, 562–583.
202. Li, J. Y. *et al.*, Lewy bodies in grafted neurons in subjects with Parkinson's disease suggest host-to-graft disease propagation. *Nature Med*., 2008, **14**, 501–503.
203. Clavaguera, F. *et al*., Transmission and spreading of tauopathy in transgenic mouse brain. *Nature Cell Biol*., 2009, **11**, 909–913.
204. Desplats, P. *et al.*, Inclusion formation and neuronal cell death through neuron-to-neuron transmission of alpha-synuclein. *Proc. Natl. Acad. Sci. USA*, 2009, **106**, 13010–13015.
205. Frost, B., Jacks, R. L. and Diamond, M. I., Propagation of tau misfolding from the outside to the inside of a cell. *J. Biol. Chem*., 2009, **284**, 12845–12852.
206. Speare, J. O., Offerdahl, D. K., Hasenkrug, A., Carmody, A. B. and Baron, G. S., GPI anchoring facilitates propagation and spread of misfolded Sup35 aggregates in mammalian cells. *EMBO J*., 2010, **29**, 782–794.

ACKNOWLEDGEMENTS. We thank members of our laboratory for discussions. J.B.U. is a recipient of a J. C. Bose National Research Fellowship from the Government of India. This work was partly funded by the Department of Biotechnology, Government of India.

Received 10 August 2011; accepted 12 October 2011